RESEARCH ARTICLE VOLCANICA

Using obsidian in glass art practice

Fabian B. Wadsworth[*α], Edward W. Llewellin[α], Colin Rennie[β], Cate Watkinson[β], Joanne Mitchell[β,γ], Jérémie Vasseur[δ], Alastair Mackie[ϵ], Fleur Mackie[ϵ], Alexandra Carr[ζ], Tobias Schmiedel[η,θ], Taylor Witcher[η], Arianna Soldati[δ,ι], Lucy E. Jackson[α], Annabelle Foster[α], Kai-Uwe Hess[δ], Donald B. Dingwell[δ], Russell J. Hand[κ]

[α] *Department of Earth Sciences, Durham University, Durham, DH1 3LE, United Kingdom.*
[β] *Department of Glass and Ceramics, University of Sunderland. United Kingdom.*
[γ] *36 Lime Street Studios, Newcastle upon Tyne, NE1 2PQ, United Kingdom.*
[δ] *Department of Earth and Environmental Science, Ludwig-Maximilians-Universität, Theresienstr. 41, 80333 München, Germany.*
[ϵ] *Copperfield Gallery, 6 Copperfield St, London, SE1 0EP, United Kingdom.*
[ζ] *Institute of Advanced Studies, Durham University, Cosin's Hall, Palace Green, Durham, DH1 3RL, United Kingdom.*
[η] *Centre for Mineralogy, Petrology, and Tectonics, Department of Earth Sciences, Uppsala University, Uppsala, Sweden.*
[θ] *TU Delft, Department of Geosciences & Engineering, Stevinweg 1, 2628 CN Delft, The Netherlands.*
[ι] *Department of Marine, Earth, and Atmospheric Sciences, 2800 Faucette Drive, 1125 Jordan Hall, Campus Box 8208, NC State University, Raleigh, North Carolina 27695, USA.*
[κ] *NucleUS Immobilisation Science Laboratory, Department of Materials Science and Engineering, University of Sheffield, Sir Robert Hadfield Building, Mappin Street, Sheffield S1 3JD, United Kingdom.*

Abstract

Glass art practice is indivisible from the material behaviour of glass at a range of working conditions, providing a direct link with the science of glass and melts. The use of non-standard, non-commercial, or natural glass compositions in art usually brings with it challenges associated with unexpected or undesirable processes, such as bubble formation and growth, liquid-liquid immiscibility, heterogeneities, and devitrification. For these reasons, natural geological compositions, including obsidian, have typically been avoided in glass art, with a few pioneering exceptions. Here, we bring together the results of mutual experimentation, knowledge-exchange workshops, and successful obsidian and magma use-cases in glass art in order to constrain the usability of obsidian and the techniques most suitable for rendering the material amenable to glass art practice. We conclude by exploring opportunities for collaboration between volcanologists and glass artists, which we propose would develop both fields in novel directions.

Keywords: `Lava; Glassblowing; Studio glass; Art and science; Minecraft™`

1 Introduction

Obsidian is perhaps the best-known natural glass. It is formed when magma crosses the glass transition without sufficient time for crystallization, and is found in cooled silicic lavas [e.g. Fink 1983] or 'high grade' and rheomorphic welded ignimbrites [e.g. Andrews and Branney 2011], at the quenched margins of silicic dykes and sills [e.g. Saubin et al. 2019], and in volcanic bombs and pyroclasts [e.g. Gardner et al. 2019]. Obsidian has been used and traded throughout human history and pre-history, with wide utility and aesthetic importance including cutting, decoration, as mirrors, and as spiritual or religious objects [Dixon et al. 1968; Chataigner et al. 1998; Tuffen et al. 2021]. Additionally, obsidian features in modern popular culture, sometimes as a material with mysterious properties, such as 'dragonglass' in the book and television series Game of Thrones where is it required to vanquish White Walkers [Martin 1996], or as a component material in the recipe required to access The Nether—a hellish underworld—in the video game Minecraft™. Due to the wide range of reference points interweaving historical, natural, human-cultural, and imagined-supernatural contexts, one might expect obsidian to be used widely as a material for art practice, and glass art practice specifically. However, there appear to be relatively few examples where this volcanic material has featured in glass art. We propose that a reason for this is that the material is typically very challenging to work with, especially in hot-glass art practice; we use this proposition as a starting point for this investigation.

The push for continual innovation in the glass art community generally leads to new challenges. While traditional glassblowing techniques require a very high level of craft skill [O'Connor 2007], many of the technique challenges associated with creating intricate forms of a range of sizes have been surmounted in the millennia since glassblowing began [Stern and Schlick-Nolte 1994]. Today, what might be thought of as the 'new frontiers' in glass art in terms of techniques, include:

*Corresponding author: fabian.b.wadsworth@durham.ac.uk

- the use of digital techniques to assist in design and with direct glass manipulation [e.g. Klein 2018] including 3D printing of cold or hot glass [Chivers 2015; Kotz et al. 2017];
- the manipulation of increasingly intricate glass-gas bubble forms and internal gas manifolds [Mitchell 2015], challenging what is possible at small or large scales;
- the use of structure or composition to impose interesting material properties such as high elastic stability under flexure;
- and the use of new materials that go beyond the soda-lime-silica or borosilicate standards (e.g. the reinvigorated use of uranium glass that glows under ultraviolet light*, glass with specific optical or textural qualities, or glass with specific devitrification rates that create interesting surface phenomena, to name a few examples), with potentially unexpected and interesting results.

Much of the push to innovate along the lines of these 'new frontiers' is driven by a push for glass art as sculpture, fine art, and conceptual contemporary art, possibly drawing distinctions with craft art, and the decorative crafting that obsidian is known for in human pre-history. Although such craft-art distinctions can be arbitrary and contentious, these are key themes for discussion in the modern glass art movement.

The range of glass-forming materials in industry, science, and nature is staggering [e.g. Martinez and Angell 2001], and yet only a narrow range of compositions are used routinely. The requirements for a glass to be used widely and routinely in industry and art include: (1) affordable cost of raw materials; (2) that the glass melt has a wide temperature range in which the viscosity remains appropriate for manipulation (the working range); (3) that the crystallization rate is low even on slow cooling, averting devitrification [Cummings 1997]; and (4) that the material is widely available or accessible (i.e. in the case of obsidian, given its scarcity worldwide, this is not a trivial issue). We propose that materials or techniques can be tweaked in order to render a wider range of compositions useable by glass artists, including obsidian. By aspiring to widen the compositional range available—specifically including natural volcanic compositions—artists may be able to draw on a wider range of conceptual touchpoints that open up new artistic possibilities and push further (and in new directions) some of those material boundaries given above.

Just as there are potential advantages for glass artists in developing methods by which obsidian might be used, the wider use of volcanic materials in glass art may be advantageous for volcanologists and volcano science research. Among many such possible advantages, the craft-knowledge associated with experimental glass art has yielded considerable advances in how bubbly glass materials can be created in bespoke 3-dimensional forms [Mitchell 2015]. These techniques involve the manipulation of gas and glass in such a way that gas can be effectively vented during fusing of glass sheets in kilns, leaving trapped gas volumes with designed shapes. This technique among others has the potential to be beneficial to experimental volcanologists who seek to replicate complex gas-magma forms found in nature, in order to better understand their properties and how they evolve in time when hot. In this Research Article, we explore the ways in which volcanic materials, and obsidian specifically, have been used in glass art practice, and we aim to draw a narrative link between the science of volcanic materials and the potential for solutions to glass art problems, while not dictating solutions to glass artists *ab excelsis*†.

1. First, we aim to constrain the working temperature range—as it is defined in glass art—for natural obsidian materials, and to explore the extent to which this may be a primary factor that has prevented wider usage of obsidian in glass art and across glass art disciplines (Section 4).
2. Second, we aim to use a particular glass art piece ('PEDM'; Figure 1) as a detailed case study, showing how obsidian material challenges can be overcome. This piece was created as an independent artwork rather than as part of this study. We use this as an opportunity to demonstrate the extent to which modern volcanological models for the behavior of obsidian in nature can provide quantitative maps for obsidian treatment in glass art workshops; thereby directly illustrating the science-art crossover potential here (Section 5).
3. Finally, we aim to examine that science-art intersection and constrain the ways in which volcanologists and glass artists can exchange knowledge for mutual benefit and direct collaboration (Section 6).

The aims stated here are taken in turn, which means that we blur the distinctions between methods, results, and interpretations. For example, in exploring the first aim, we use some experimental methods and interpret the results thereof, before moving on to the second aim, and so on.

2 Terminology, and translating between glass art and volcanology

In Table 1, we curate a selected list of terminology used frequently in glass art disciplines. These terms are

*See Colin Rennie's *Beyond the Visible*: https://www.colinrennie.co.uk/beyond-the-visible

†*Ab excelsis* approximately translates as 'from on high'

Table 1: A glossary of terms for dialogue between glass artists and volcanologists.

Glass art term and definition	Analogous volcanology process or term
Frit (sometimes called granular glass). Angular crushed glass particles at diameters <2 mm.	Analogous to non-porous volcanic ash particles (albeit with textural differences).
Soak. An isothermal hold time in a furnace or kiln.	Isothermal hold.
Seed. The nucleation or trapping of small bubbles at high temperature.	Vesiculation or bubble nucleation and growth.
Stones. Lumps of crystalline material that tend to sink in molten glass.	Lithics/cumulates/enclaves.
Soft/strong glass. Soft glass is one with a low glass transition temperature or low temperature working range relative to a soda-lime-silica standard art glass. Similarly, a strong glass is one with a high relative glass transition temperature.	Low/high glass transition temperature (or low/high general working range) compared with a standard glass (probably a soda-lime-silica glass).
Short/long glass. A short glass has a steep temperature-dependence of viscosity measured at the glass transition temperature, resulting in a 'short' working range of temperature. A long glass has a shallow temperature-dependence of viscosity. This is equivalent to fragile/strong descriptions used in the main text [Angell 1995].	High/low slope of the temperature dependence of viscosity around the glass transition temperature.
Architectural tint or coloration. A tint imparted during float glass formation on a dense liquid metal. Coloration can occur during post-float re-heating. Tints can be also be produced post-float by re-melting the glass and dissolving in additional compounds.	Metal diffusion.
Crawl or creep. The loss of bulk volume during sintering and casting processes.	Densification.
Devitrification. The crystallisation of glass between the liquidus and the glass transition interval.	Devitrification.
Compatibility. The measure of how close is the thermal expansivity of two glass compositions when fusing them; poor compatibility is manifest as fracture propagation in one of the glasses on cooling.	Differential expansion.
Pâte-de-verre. A process of (1) mixing glass particles with a liquid to form a concentrated particle suspension, (2) applying the suspension to a surface, and (3) firing the surface to evaporate the liquid and sinter/fuse the particles. The liquid used is typically a cellulose solution or similar.	Welding.
Powder printing. Sintering/fusing a single or bi-layer of glass particles on a surface in a given pattern.	Welding/coalescence.
Enamelling/Lustreing. Sintering/fusing fine glass powders to surfaces producing a smooth finish. While enamel is glass- or ceramic-based, lustres are metal-based.	Welding.
Fusing. Joining two plates, slabs, or surfaces of glass together by softening the glass at high temperature.	Fracture-healing.
Crackle. Exploiting differential expansion and viscoelasticity during glassblowing to produce a crackled surface texture while hot.	Fracture-healing on bubble surfaces.
Cord. Streaks in glass, which are undesirable in some situations (e.g. during glassblowing) but may be produced by design in other situations.	Diffusive trails behind rising bubbles.
Veiling. Bubbles trapped in former fracture or suture interfaces.	Fracture-healing with trapped vesicles.
Squeeze. Reducing the temperature of a pot or crucible of hot glass in order to remove seed via thermal resorption due to the increase in solubility of most gases on cooling.	Thermal bubble resorption.

either collated from published sources [Halem 1996; Cummings 1997; Schmid 1998; Petrie 2019] or via discussion with practicing glass artists. We select terms that have some analogy in volcanological processes or volcanic materials, and then provide a loose working definition of the term.

The terms 'obsidian', 'pitchstone', and 'perlite', bear inconsistent definitions in published work, and are each in some way used to relate to volcanic glass. 'Pitchstone' and 'perlite' often are used to refer to rocks that may have hydrated substantially by secondary processes (pitchstone), and/or developed a conchoidally finely cracked texture associated with hydration [perlite; De Campos and Hess 2021]. While these terms are all generally used for natural silicic glass in the composition region from rhyolite to phonolite [and sub-fields therein; Tuffen et al. 2021], there are occurrences of usage of 'obsidian' to refer to natural glass across the compositional spectrum of glasses in magmatic systems. Similarly, Studio Drift* use 'obsidian' in art to refer to the quenched glass product of melting waste materials outside of a volcanic genetic context. Here we restrict our usage to 'obsidian' throughout and use this to mean silicic volcanic glass only. Furthermore, we suggest that for most material uses, hydrated pitchstone or hydrated and cracked perlite may be more challenging to use in glass art and that young or 'fresh' obsidian may be more readily utilized.

3 Glass art and volcanology

The use of glass as a material in sculptural art is long-lived [e.g. Lukens 1965; Kunz and Mills 2021]. However, the so-called 'studio glass movement' represents a relatively recent re-popularization of traditional glass-working methods, along with a rapid expansion of experimental, innovative, and modern methods, often embracing science techniques and equipment. This studio glass movement started in the 1960s and is characterised by the use of glass as a medium of artistic expression. Since this movement, glass has emerged as a significant part of general art and design practice worldwide. The use of glass in art could be divided into (1) architectural glass practice, (2) kiln-formed glass practice, and (3) hot glass practice [Petrie 2019]. In general, in terms of the making process, these subdivisions map onto (1) low, (2) medium-to-high, and (3) high-temperature glass working (specific temperature ranges constraints are discussed in Section 4). Architectural glass practice covers a broad array of work using flat glass panels or pieces that are printed, painted, etched, cut, joined, ground, and sandblasted. Kiln-formed glass practice involves the use of closed kilns to heat molds or assemblages of glass to fuse, sinter, cast, bend, stretch, print, anneal, and enamel glass before cooling again [Cummings 1997; Petrie 2019]. Finally, hot glass practice involves the use of molten glass directly from a furnace and typically involves glassblowing, but may also involve other manipulation techniques and types of direct casting or pouring, and lamp- or flame-work. We note that this grouping of glassblowing with casting and lamp- or flame-work may not be universally accepted and that, strictly speaking, these are distinct disciplines; however, for the purposes of this study, divisions along the lines of hot- vs. cold-working are convenient as a working classification system. Taken together, glass art practice involves a truly vast array of physical processes, such that the craft skill of the glass artist is in harnessing or embracing these processes for desired effects. In modern industrial glass processing and glass production, a similar range of physical processes are at work, although there are additional processing challenges that come with large spatial scales of production and the demand for reproducible precision [Mouly 1969].

In the Earth Sciences, early experimental work by the first experimental igneous petrologists began in industrial kilns and furnaces not dissimilar to those used by glass artists [Newcomb 2009]. This is a testament to the similarities extant between the range of conditions that can be achieved in a glass artist's workshop and those found in volcanoes [Wadsworth et al. 2019a], and to the similarities of material composition: both the glasses used in glass art and the melt phase erupted in most volcanoes on Earth are subsets of the wider silicate glass family of materials [Cicconi and Neuville 2019; De Campos and Hess 2021]. While there are important differences—not least the absence of elevated confining pressure conditions in most glass art—there are striking similarities between many volcanic processes and many of the glass art processes in all of the architectural, kiln-formed, and hot glass sub-practices. In all cases the materials readily flow, vesiculate, fracture, heal, anneal, cool conductively, variably crystallize, and granulate. While a glass art process may not be an exact replication of a volcanic process in terms of the precise temperatures, pressures or material compositions used, there often exists a dynamic similarity, such that it is in the same physical *regime*, with the same broad phenomena manifesting in the material behavior. Similarly, this implies that there exists a mathematical scaling between any description of the glass art and analogous volcanic processes in question. A central aim of this article is to explore that dynamic similarity when comparing the behavior of obsidian and the behavior of glass compositions used in hot glass studios.

3.1 Examples of obsidian use in art

Obsidian has been used in glass art in a number of different ways. These examples can be coarsely divided into cold-worked obsidian, and hot- or kiln-worked obsidian. In this context, cold-working refers to the suite of methods by which obsidian would be polished,

*https://studiodrift.com/work/the-obsidian-project/

cut, shaped, mounted, and manipulated without the application of heat sufficient to cause flow. By contrast, hot- and kiln-working refers to glass manipulation through the application of heat sufficient to induce partial or complete glass flow and the myriad resultant processes that can result from that change. The cold-working category bears some analogy with the architectural glass category described earlier (Section 3), however, there are key differences discussed here.

Modern cold-working of obsidian is reminiscent of early obsidian manipulation for the production of jewellery, mirrors, and knapped cutting tools. An example of obsidian cold-worked in art is 'Monolito' by Eduard Olbes, in which a large block of obsidian from Hidalgo, Mexico, was polished and shaped into the final piece (Figure 1A). 'Monolito' is an exceptional example of pristine natural glass apparently free from obvious surface defects. This is somewhat unusual for obsidian, which is more typically heterogeneous, with microstructural features that reflect the complexities of its formation mechanism [Tuffen and Dingwell 2005]. By contrast, in 'Thickens, pools, flows, rushes, slows' by Julian Charrière (Figure 1B), large pieces of heterogeneous and flow-banded obsidian are set in a gallery context with cold-worked concave polished sections, which resemble large volcanic vesicles. Perhaps the best known cold-worked obsidian is the mirror used by the 16th century mathematician and occultist, Dr John Dee, which is thought to have been originally worked in Aztec culture, Mexico [Ackermann and Devoy 2012; Tuffen et al. 2021].

Examples of kiln- or hot-worked obsidian include 'Gravity Pull' by Matt Durran in which heterogeneous natural obsidian collected from an unknown volcano was heated until it vesiculated, before being cooled. The result of this treatment is to render it positively buoyant in water (Figure 1C). The creation of Durran's piece uses the natural process of exsolution of the dissolved volatiles in obsidian at temperatures above the glass transition temperature [c.f. Prousevitch et al. 1993; Coumans et al. 2020], in order to manipulate the glass artistically. Other examples, such as Variation 1 of 'Variations on an energetic field' by Lucy Bleach (Figure 1D) and 'PEDM' by Alastair Mackie (Figure 1E), are created using hot-working methods specifically designed to avoid the vesiculation that Durran exploited. In the making of 'PEDM', crushed obsidian (from Roche Rosse, Lipari, Italy) is heated and vesiculated to equilibrium, effectively dehydrating it, before being cooled and re-crushed. The resultant powder is then the raw material for the work. The artist—Mackie—used a technique to sinter the dehydrated obsidian in a mold of desired shape (explored in detail in Section 5). In the case of 'Variation 1', Bleach sintered obsidian particles mixed with so-called impact glass [Darwin impact glass; Fudali and Ford 1979] to completion, resulting in a dense glass sheet.

3.2 Challenges of obsidian use in art

While there are other examples of obsidian in art, those given here provide an overview of a range of approaches to obsidian glass art in both cold- and hot-working. The examples also demonstrate that artists take different approaches to overcoming the challenges associated with using obsidian. One such challenge is dealing with the ubiquitous remnant volatile H_2O [Castro et al. 2012; Wadsworth et al. 2020] that renders typical rhyolitic obsidian supersaturated at 1 bar pressure (atmospheric pressure) and elevated temperatures $\gtrsim$800 °C [Liu et al. 2005], and thus prone to vesiculation when heated to working temperatures. In the case of Durran's piece (Figure 1C), this material challenge was used to the artist's advantage, such that the formation of bubbles and the resultant gas-derived buoyancy of formerly high-density obsidian, becomes central to the piece. That is to say, Durran did not attempt to surmount the material challenges of obsidian, but embraced them instead, utilizing them for conceptual impact to surprise the viewer. By contrast, Bleach and Mackie found methods by which this same challenge of the excess H_2O in obsidian could be overcome prior to the production of a final piece. Mackie applied a pre-making processing step to refine obsidian by removing the excess H_2O; their process is discussed in detail later (Section 5). Olbes and Charrière took a third approach: by selecting a piece of starting obsidian that was especially suited to the work prior to beginning the piece, they were able to minimize the alteration of its state induced by cold-working. Olbes therefore selected the piece with the minimum of attendant material issues to overcome and Charrière selected the pieces with a natural heterogeneity, which he could offset against the cold-worked concave components.

Another challenge, encountered in hot-working of obsidian, is that its working temperature range is rather different from that of artistic glasses. The paucity of examples of hot-working of obsidian that use traditional glassblowing techniques likely stems from this difference.

4 Art glass vs. obsidian: The working temperature range

For all glasses there is a temperature range over which the glass melt is workable which impacts both commercial production and artistic practice. This temperature range is determined by the viscosity-temperature relationship and thus the composition of the melt, as well as the process being used. Too hot, and the glass melt will flow too quickly for the artist to react or manipulate it; too cold, and the glass will not flow even under large applied forces from the artist. Therefore, temperature is a key constraint on the glass artist and their ability to achieve a given result with a particular

Figure 1: Examples of obsidian in modern glass art. [A] 'Monolito' by Eduardo Olbes; cold-worked, polished obsidian. [B] 'Thickens, pools, flows, rushes, slows' by Julian Charrière; cold-worked, partially polished obsidian (at Aargauer Kunsthaus, Aarau, Switzerland, 2020). [C] 'Gravity's Pull' by Matt Durran; partially vesiculated obsidian. [D] Variation 1 of 'Variations on an energetic field' by Lucy Bleach; a thoroughly welded obsidian sheet. [E] 'PEDM' by Alastair Mackie; obsidian partially welded in a mold.

glass. Similarly, in volcanic eruptions, temperature is a first-order control on the behavior of magmas at a given volcano. For many processes the working viscosities of glass lie between 10^3 and 10^8 Pa s [Mouly 1969]. This range of working viscosities may be wider when considering all of the possible processes that fall under glass working, including lower temperature processes such as bending.

For kiln-forming, Cummings [1997] proposes six stages, each relating to a progressively higher temperature window. In Stage 1 at 450–550 °C, the surface layer of a glass can become 'mobile' or relax and enamels and metallic lusters can be bonded to it. In Stage 2 at 550–650 °C, unsupported glass will bend under its own weight and take up simple forms by slumping or folding. In Stage 3 at 650–750 °C, glass will deform readily under gravity and can be stretched under the force of a tool or gloved hand. In Stage 4 at 750–850 °C, pieces of glass can be fused together and glassblowing using a blowpipe is possible. In Stage 5 at 850–900 °C, so-called inert casting is possible, and casts or molds filled with glass particles will densify and take the form of the mold (often with the requirement that the glass is topped up to accommodate the decrease in overall volume during sintering/casting). Finally, in Stage 6 at 900–975 °C, so-called mobile casting is possible where casts, molds, containers, reservoirs, and crucibles will fill with liquid glass readily and areas of relatively tight curvature can be filled directly with molten glass pours. Cummings [1997] suggests that temperatures greater than 975 °C are not to be used, presumably due to effects such as volatilization, crystallization, sticking of glass to molds, thermal breakdown and brittleness of mold materials, among others. Similarly, but more coarsely, Volf [1961] propose that for hot-working, 700–900 °C is the so-called 'working range' (ibid. p.72–74).

While such temperature ranges are useful general guides for users, they are not universal to all glasses as different glass melts can have markedly different viscosity-temperature relationships with the melt viscosity of so-called 'long' or 'strong' glasses increasing more slowly with decreasing temperature than that of so-called 'short' or 'fragile' glasses. The use of specific temperature ranges in glass art guide texts therefore comes with an assumption that glass artists are using standard compositions that are common discipline-wide (although Cummings' text does indicate that

different annealing profiles are required for different glass types). In almost all cases, the composition used for glassblowing will fall into the soda-lime-silica glass compositional family. Indeed, it is this composition that is assumed when quoting specific temperature ranges for specific working practices (see above). However, for lamp- or flame-work (i.e. using an oxy-acetylene or propane torch to heat and manipulate smaller rods and pieces of glass), borosilicate glass is often used in place of soda-lime-silica compositions. The change in composition from soda-lime-silica to borosilicate is sufficient to increase the upper working temperature by some 100 °C, to >800 °C.

The rate at which the internal stresses in a glass are substantially relieved by relaxation depends on temperature. Stress relaxation takes place in a few minutes at the glass transition temperature T_g, whereas at the strain point the internal stresses are only relieved by relaxation after several hours. The strain point is typically taken to correspond to a viscosity of 1013.5 Pa s. Therefore, constraining T_g, and the temperature-dependence of the viscosity $\mu(T)$ around T_g are two fundamental measurements required to assess the workability of a given glass. Other temperatures used in glass art—such as the annealing points—can be estimated using $\mu(T)$. In this section we investigate experimentally the flow behavior of obsidian liquids at high temperature without suspended bubbles. We compare this flow behavior with a typical glass used for glass art purposes under the company name Cristalica® and a standard borosilicate used in glass art.

Table 2: The bulk composition of the glass used here expressed as weight percent major oxide components.

Oxide component	Cristalica® wt.%[a]	Obsidian wt.%[b]
SiO_2	69.0–71.5	75.17
TiO_2	-	0.22
Al_2O_3	1.1–1.5	12.02
FeO	-	3.13
MnO	-	0.11
MgO	-	0.09
CaO	4.0–4.5	1.66
Na_2O	12.5–12.9	4.58
K_2O	5.0–5.5	2.88
BaO	2.5–3.0	
B_2O_3	1.0–1.5	
ZnO	0.6–1.3	
Sb_2O_3	0.2–0.5	
H_2O[c]	n.d.[d]	0.14
Totals	95.9–102.2	99.86

[a]Data from Cristalica® datasheet via KutaGlass and for 'Premium Studio Glass 100' batch. Note: omitted here are trace concentrations of Li_2O and Er_2O_3. Normalisation is nominal given the uncertainty ranges from reproducibility effects associated with large batch production.
[b]Data normalised from Tuffen and Castro [2009].
[c]H_2O data is consistent with the results presented in Tuffen and Castro [2009] but is derived via viscosity determinations made herein.
[d]Cristalica® is nominally anhydrous, although we note that trace amounts of H_2O are impossible to avoid during glass mass production by most techniques.

4.1 The glass transition interval T_g

We used a Netzsch Pegasus 404c simultaneous thermal analysis tool to analyze two glasses: Cristalica®, and obsidian from Hrafntinnuhryggur at Krafla volcano, Iceland [Tuffen and Castro 2009]. The composition of the glass used here is given in Table 2. A 30–50 mg chunk of each glass was held in a lidded platinum crucible and heated at a constant rate in argon. Via this technique, we measure the heat flow (in this case recorded as a voltage in a thermocouple array) at the base of the sample crucible, relative to the heat flow at the base of an empty reference crucible. We performed runs with new samples, heating them at 0.4 °C s^{-1} to temperatures around 650 °C (Cristalica®) or 850 °C (obsidian), before cooling them at 0.4 °C s^{-1} again. This first heating run results in relaxation of the glass and eradicates the thermal history associated with manufacture (Cristalica®) or cooling in nature (obsidian). Then subsequent heating runs were performed on the same sample at different pairs of heating and cooling rates, designed such that the cooling rate from the previous run matches the heating rate of the next run. This thermal analysis allows us to find the onset and the peak of the glass transition interval below which the glass is a solid and above which the glass can relax in response to applied stresses viscously. This technique of matched cooling-heating runs allows us to observe the dependence of the glass transition on the rate of temperature change [Wilding et al. 1996; Gottsmann et al. 2002].

In Figure 2, we show the heat flow curves on heating for Cristalica® and obsidian, omitting the first heating run. The curves are for different heating rates q. We use arrows to mark the onset and the peak of the glass transition interval. We note that the first-order finding is that Cristalica® relaxes via the glass transition interval at significantly lower temperatures than obsidian, as we would expect from its composition [Angell et al. 2000].

4.2 Viscosity

The viscosity of silicate liquids can vary over many orders of magnitude across the range of temperatures typical of both volcanic processes and artistic practice [Angell et al. 2000; Fluegel 2007; Giordano et al. 2008]. For this reason, we deploy a number of techniques to constrain the temperature dependence of viscosity across the relevant range.

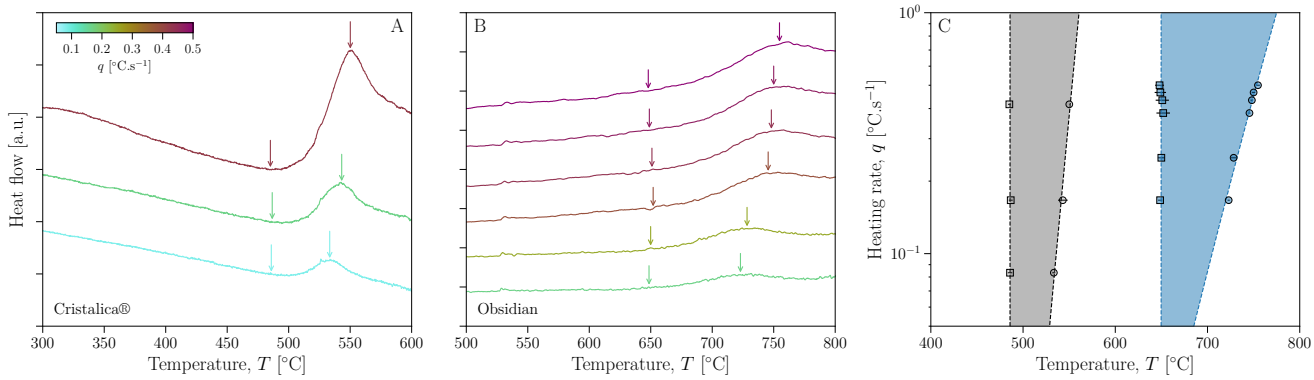

Figure 2: Structural relaxation of [A] synthetic Cristalica® glass used by glass artists, and [B] natural obsidian from Hrafntinnuhryggur, Krafla, Iceland, measured by differential scanning calorimetry at constant heating rates, yielding temperature-dependent heat flow curves (see text). In [A] the curves are for 3 heating rates: 0.08, 0.167, and 0.42 °C s^{-1}; in [B] the curves are for 6 heating rates: from 0.167 up to 0.467 °C s^{-1}. The arrows denote the onset and peak (from left to right) of the glass transition interval, where the onset is measured as the first deviation from a linear baseline [see Gottsmann et al. 2002]. [C] The window between the onset and peak of the glass transition interval for Cristalica® (grey) and obsidian (blue). Note that the temperature position of the peak is heating rate dependent.

First, using semi-empirical models for the relationship between relaxation and viscosity, we can use the temperature at which the peak of the glass transition interval occurs (Figure 2) to constrain the viscosity at the glass transition. Gottsmann et al. [2002] shows that the viscosity at the glass transition temperature $\mu|T_g$ and the heating rate at which the glass transition temperature is determined are related via a constant c (with units of Pa K), where c is a weak function of the glass composition

$$\mu|T_g = \frac{c}{|q|}. \quad (1)$$

Gottsmann et al. [2002] provide an empirical model for relating c to the composition, showing that c is controlled dominantly by the wt.% cations in the melt that are excess to the charge balancing roles dictated by the network forming cations. The Gottsmann et al. [2002] empirical model for predicting c results in $c = 6.17 \times 10^9$ Pa K for Cristalica® and $c = 2.51 \times 10^{10}$ Pa K for the obsidian [where the obsidian composition is taken from electron microprobe measurements presented in Casas et al. 2019]. Equation 1 therefore yields values for μ at $T = T_g$ for the high-viscosity end of the full working range (Figure 3).

To constrain the viscosity at temperatures above the glass transition interval, other techniques are required. Here we supplement the data derived from Figure 2 with constraints using a rotational rheometer in which crushed chunks of each glass are loaded into large platinum crucibles and held at high temperature (1300 °C for Cristalica® and 1400 °C for the obsidian) for 12 hours, ensuring homogenization to a single-phase liquid. A platinum-coated spindle [Dingwell and Virgo 1988] is lowered into the melt and controlled using a Brookfield HBTD which can apply rotation speeds of 0.5–50 rpm. The apparatus, technique, and data processing are described by Dingwell [1989]. The technique involves a series of temperature reduction steps, rotating the spindle until the measured torque equilibrates at each temperature before moving to the next. The equilibrium torque is then proportional to the shear stress, which together with the rotation rate, can be used to compute the shear viscosity. In Figure 3 these data for both the obsidian and the Cristalica® glass occupy the high-temperature end of the curves.

At temperatures intermediate between the glass transition interval and the high temperatures of the rotational rheometry, we apply a so-called micro-penetration technique [Pocklington 1940; Tobolsky and Taylor 1963]. This involves determining the rate at which an iridium indenter displaces the melt when a fixed load is applied. These measurements were applied to the obsidian, which was cut to 3 mm long plane-parallel discs of 5 mm diameter and polished on both surfaces. The sample is placed in a Netzsch 402 F1/F3 Hyperion thermo-mechanical analyzer under argon gas flow and the indenter is attached to the vertical push rod. The viscosity is then determined from

$$\mu = \frac{\gamma F t}{\sqrt{r\alpha^3}} \quad (2)$$

where $\gamma = 0.1875$ is a dimensionless constant for a hemispherical indenter, F is the applied force, t is the time since contact of the indenter, r is the indenter radius (1 mm in this case) and α is the time-dependent distance into the silicate liquid [Pocklington 1940; Tobolsky and Taylor 1963]. Viscosity μ is taken at steady-state (large t for which $d\alpha/dt$ becomes constant).

Finally, these data are supplemented with (1) data from the company datasheet supplied with Cristalica®

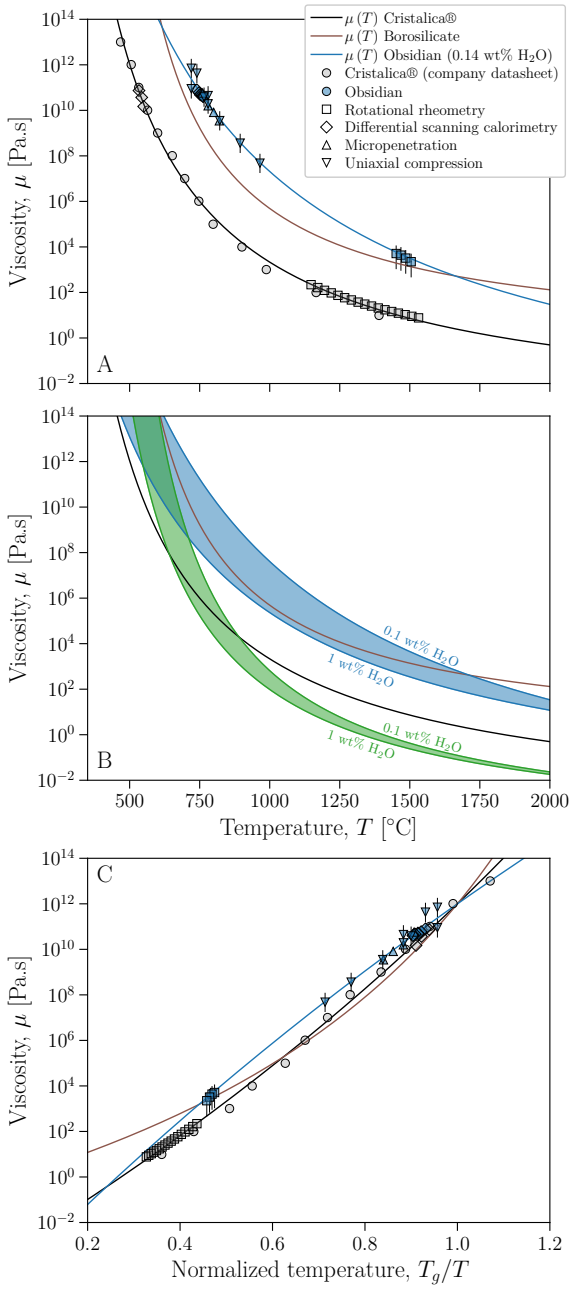

Figure 3: The viscosity of glass melts. [A] The temperature dependence of viscosity of Cristalica® and obsidian. Error bars are given as vertical lines through the data points where an experimental uncertainty is larger than the size of the data point. [B] A comparison between the viscosity of the glass melts studied here and the temperature dependence of viscosity for metaluminous rhyolite (blue region) for 0.1 and 1 wt.% dissolved water concentration via a constitutive model [Hess and Dingwell 1996] and the temperature dependence of viscosity for a basaltic composition (green region) using a model for hydrous Etna composition [Giordano and Dingwell 2003] for 0.1 and 1 wt.% dissolved water concentration. [C] The normalized viscosity via the method given by Angell [1995].

glass*, (2) a 'viscosity curve' for a standard borosilicate glass [Napolitano and Hawkins 1970], and (3) data from a cylinder compression technique described by Gent [1960] and applied at high temperature to the same obsidian used herein by Wadsworth et al. [2018].

Taken together, the constraints given above provide $\mu(T)$ data covering a wide range of temperature. To these data, we fit the widely-used Vogel-Fulcher-Tamman equation [Lakatos et al. 1972; Lakatos 1976; Angell et al. 2000; Giordano et al. 2008]:

$$\mu = \mu_0 \exp\left(\frac{B}{T - T_0}\right) \tag{3}$$

where μ_0, B, and T_0 are all empirical fit parameters; for glasses of commercial interest standard compositional parameters have been empirically determined [Lakatos et al. 1972; Lakatos 1976; Fluegel 2007]. Our fit procedure uses the least squares regression method on data for $\log(\mu)$, fitting the logarithmic form of Equation 3. For Cristalica® we find the best fit to Equation 3 with $\mu_0 = 2.73 \times 10^{-4} \pm 1.45 \times 10^{-4}$ Pa s, $B = 14230.82 \pm 810.06$ °C, and $T_0 = 103.74 \pm 17.91$ °C and for the borosilicate we find good agreement with $\mu_0 = 0.52$ Pa s, $B = 9239.12$ °C, and $T_0 = 328$ °C (Figure 3A). For obsidian, there exists a multi-component viscosity model calibrated for calc-alkaline obsidian, for which these fit parameters are taken to be a function of the dissolved H_2O concentration in the glass structure [Hess and Dingwell 1996]. Using the Hess and Dingwell [1996] model, we find good agreement between our obsidian data for $\mu(T)$, and the model result for 0.14 wt.% H_2O in the glass. This best-fit H_2O concentration is, in turn, consistent with direct H_2O determinations using this same obsidian [Tuffen and Castro 2009; Ryan et al. 2015; Wadsworth et al. 2018; Coumans et al. 2020; Seropian et al. 2022; Weaver et al. 2022].

The viscosity-temperature curves for obsidian and Cristalica® appear to converge in the low temperature region around 550 °C for obsidian with a relatively high dissolved H_2O concentration of 1 wt.%. However, for the more common obsidian with a dissolved H_2O concentration around 0.1 wt.%, such as that tested herein, rhyolitic obsidian has a higher viscosity than Cristalica at any given temperature over the interval investigated (Figure 3A). By contrast, natural obsidian across the range of dissolved water concentration 0.1–1 wt.% has a similar range of viscosities for a given temperature to borosilicates, such as those used in lamp- or flame-work (Figure 3B). Cristalica® shares more similarities, in terms of viscosity-temperature behaviour, with a basaltic magma, particularly in the range of temperature 600–1000 °C (viscosity range approximately $10^4 < \mu < 10^8$ Pa s). The basaltic viscosity-temperature relationship is found using a hydrous Etna composition as indicative of a basaltic glass [Giordano and Dingwell

*https://cristalica-studioglass.com/Datenblatt/

2003]. Unlike obsidian, sub-aerial, terrestrial basaltic glasses are relatively unstable and prone to crystallization, and so while the comparison is tantalizing, basaltic glass is unlikely to be of wide utility in glass art.

4.3 Strong and fragile glass melts: The Angell [1995] plot

Using the data described in Section 3.2, we can apply a normalization step for comparing $\mu(T)$ of silicate glasses across compositions. Angell [1995] proposed that T_g can be approximated by the temperature at which the viscosity is 10^{12} Pa s, and that normalizing all temperature values by this single T_g approximation, renders $\mu(T)$ comparable even for systems with very different T_g. Here we apply this approach using the $\mu(T)$ fits of Equation 3 to each dataset (Figure 3A) to find the value of T that corresponds to $\mu = 10^{12}$ Pa s, which we take to be T_g. In a plot of $\log\mu(T_g/T)$, Angell [1995] highlighted the difference between an Arrhenian straight-line relationship and a non-Arrhenian curved relationship. They termed glass melts that approximately follow a simple Arrhenian relationship across the entire temperature range 'strong' melts, and those that deviate significantly from a simple Arrhenian relationship 'fragile' melts.

In Figure 3C, we show the data from Figure 3A transformed in the manner described above. We find that a relatively dry (0.1 wt.% H_2O) obsidian glass melt is strong, while Cristalica® is comparatively fragile, and the borosilicate more fragile still. The practical application of this analysis is to demonstrate that, while there is an apparent similarity between the borosilicate and obsidian compositions compared with Cristalica® (Figure 3A), for a given change in temperature, the relative change in the viscosity of the borosilicate is actually more similar to Cristalica®. Given that much of active hot glass work involves changes in temperature during working, this insight into the relative pace of change of viscosity as a glass composition moves up or down temperature is crucial to building an intuitive understanding of the relative workability.

4.4 Summary: The effective working window of obsidian vs. studio glasses

The working range of viscosity for hot glass work described earlier was 10^3–10^8 Pa s [Mouly 1969]. Using the results given here we can refine this broad estimate of the working window and convert it to temperature ranges for each glass considered. We take the scheme given for kiln-forming [Cummings 1997] as a guide to how particular glass art processes (e.g. bending, stretching, fusing etc.) partition into viscosity and temperature windows. For example, if we take the temperature range given for soda-lime-silica glass for different glass art processes by Cummings [1997], we can use Figure 3A and the solution for $\mu(T)$ for Cristalica® glass from Equation 3 to assign each temperature range an associated viscosity range. If we then assume that the viscosity range is in fact the parameter that controls the workability for a given process (e.g. the ability to bend or to stretch a given glass), then we can also use Equation 3 to show what the equivalent temperature range for those processes would be for other glass melt types: i.e. for the borosilicate or the obsidian studied here.

In Figure 4, we apply the workflow described here to define a working range for different glass art processes using Cristalica®, the borosilicate, and the obsidian. This confirms what is shown in Figure 3B, that the obsidian has a high and large working temperature range relative to Cristalica®. This increase in the temperatures associated with any particular glass art process is potentially a part of the reason that obsidian has not been used more widely in glass art. However, because the working range is more similar to a borosilicate glass that is typically used in lamp or flame-work, we conclude that obsidian may be readily used in such higher temperature work. Similarly, casting or fusing processes which occur in a kiln are easily 'scaled up' to hotter temperature programs during fabrication, and may therefore be appropriate for use with obsidian.

5 The science of a case study art piece: Constraining the technical production of obsidian art

We take 'PEDM' by Alastair Mackie (Figure 1E) as a case study, which we explore in more detail. We document the process of making that was taken to create the piece and interpret and constrain the physical processes extant in the making. We posit that this process represents a form of best-practice for using obsidian in glass art and is the basis on which we recommend that casting techniques are well-suited to obsidian as a material, compared with other hot-working techniques.

5.1 Analysis of the making of 'PEDM': A work flow for using obsidian

Obsidian from the Roche Rosse deposits (Lipari, Italy) was used as the raw material for 'PEDM'. The obsidian was broken into chunks a few millimeters across (Figure 5A), and then loaded into alumina crucibles. The crucibles were then heated to 1200 °C in a furnace in air and held for 24 hours. After cooling back to room temperature, the crucibles were cut in half (Figure 5B), revealing a highly vesicular, porous glass. This porous glass was chipped out of the crucible container using hard tools, then crushed to a powder of particles with average 10–100 µm diameter (estimated). A test batch of this second powder was then poured into the base of another alumina crucible and heated once more to the

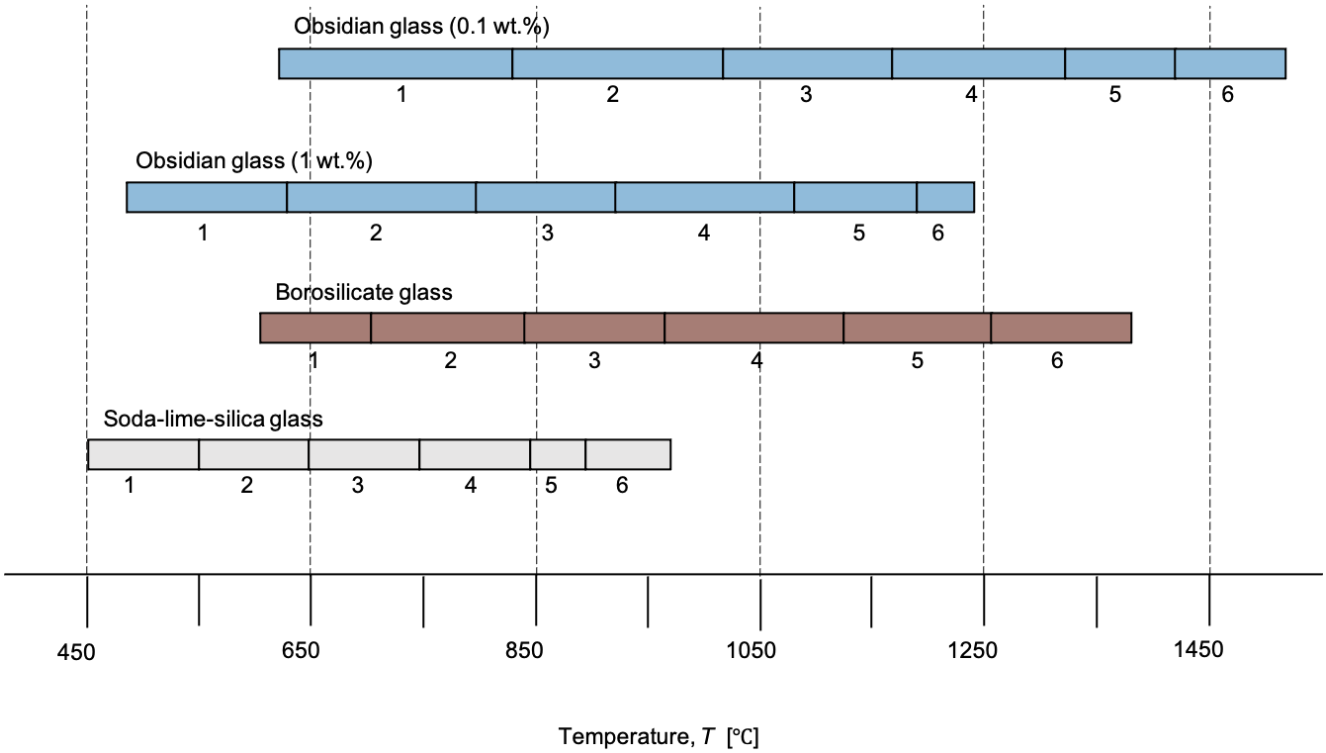

Figure 4: A summary of the working range of Cristalica® (grey), borosilicate (brown), and obsidian (blue) for each of the six processes described by Cummings [1997]: (1) enameling and lustreing; (2) bending; (3) stretching; (4) fusing; (5) casting (inert); (6) casting (mobile). The value 1.0 wt.% and 0.1 wt.% for the obsidian refer to the dissolved water concentration remnant in the glass at the time of working, such that the 0.1 wt.% obsidian refers to the glass typical of laboratory use, particularly after the processing steps outlined here (see Section 4).

same temperature for the same time. The result was a shiny pool of black glass (Figure 5C). After this test, the powder was then loaded into a bespoke mold created in the shape a hand by the artist. The mold was heated to 1200 °C and held for 2 hours (see Figure 5D for the post firing mold top). After cooling, the plaster was removed from the mold lining, revealing the final form, which was polished and finished by the artist.

In the making process involved in forming 'PEDM', there are two key processes that occur, each during the individual high-temperature steps involved. First, large chunks are heated and bubbles grow, removing dissolved H_2O from the obsidian. Second, post-bubble-growth obsidian is crushed to a finer powder (*frit*; Table 1) and this is heated in a mold and sintered to a desired degree. This latter process is a type of casting in which crushed glass is added to a mold and sometimes topped up during firing to accommodate the volume loss during sintering.

One of the key challenges that obsidian presents when used in glass art is that bubbles grow readily. For most applications, this is an undesirable effect. Even obsidian with nominally low-H_2O concentrations in the glass will nucleate and grow bubbles if heated to a temperature sufficient to result in H_2O supersaturation. For example, when the same obsidian used for viscosity determination (see Section 3) is heated to $\gtrsim$1000 °C, bubbles nucleate and grow and a piece of the obsidian will expand [Ryan et al. 2015; Coumans et al. 2020]. This occurs because the solubility of water at atmospheric bulk pressure is a negative function of temperature, such that as temperature increases, the solubility decreases [Liu et al. 2005]. To avoid bubble formation and growth, an artist could operate at temperatures that are sufficiently low to be below the solubility curve for rhyolitic obsidian, such that the material is under-saturated in H_2O. However, for the obsidian tested here, with 0.14 wt.% H_2O (Section 4), this would mean working at $T < 1050$ °C, which is below the working range for many processes including casting. The alternative approach, used in the making of PEDM, is to dehydrate the obsidian in a pre-processing step, by allowing bubbles to grow, before cooling and re-crushing the glass and using that new glass in the piece or work. This process will also aid homogenization of the material.

5.1.1 *A maker's guide for dehydrating obsidian as a pre-processing step*

Pre-processing obsidian to dehydrate it, as the artist did during the making of 'PEDM', requires that the glass is held at elevated temperature for sufficient time to allow complete degassing to equilibrium H_2O con-

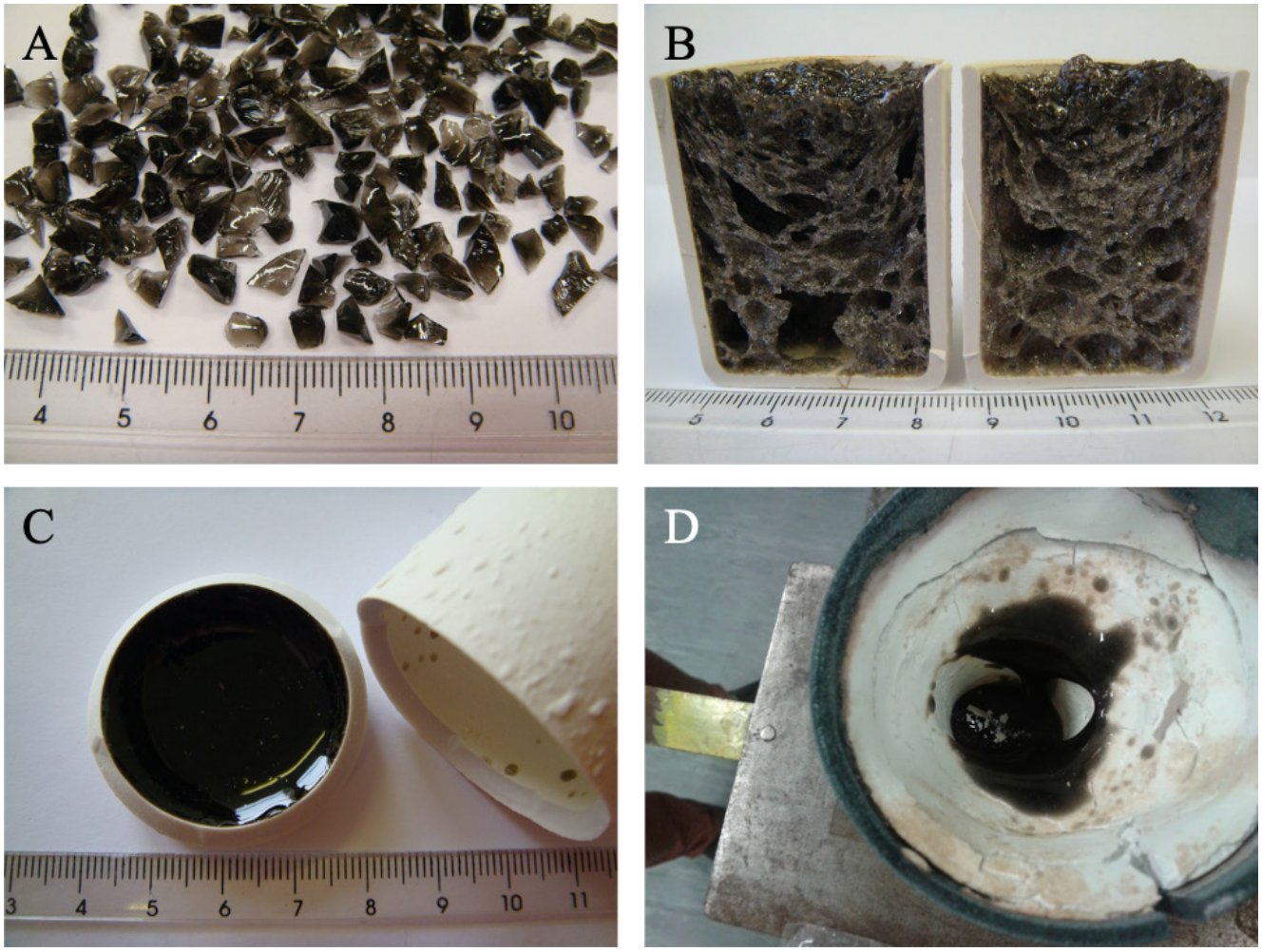

Figure 5: Photographic notes from the experimentation and making process during the production of 'PEDM' (Figure 1C). [A] The starting obsidian (from the Roche Rosse lavas, Lipari, Italy) crushed to 2–3 mm chips. [B] The obsidian chips after a processing step involving heating in alumina crucibles to 1200 °C for 24 hours. [C] The result of the second heating step in which the product shown in [B] is crushed to a fine powder and then reheated in a crucible, producing a densely welded obsidian glaze. [D] The top-view of the mold after firing.

tent (in this context 'degassing' refers to the exsolution of H_2O into bubbles and the diffusive removal of H_2O from small particles into the open-system interparticle pore spaces). In order to provide a map for pre-degassing obsidian ready for use, we use a model developed by Coumans et al. [2020] which calculates the rate of growth of bubbles of H_2O that form when obsidian is heated. The model outputs the time-evolution of the fraction of the material volume that is gas bubbles—termed ϕ—based on the input parameters. Key parameters that must be known *a priori* are: (1) the bubble number density (the number of bubbles per unit volume N) that is likely to form during bubble nucleation; (2) the temperature of the isothermal dwell at which the obsidian will be held (and ideally, temperature-time pathway *en route* to that isothermal temperature); (3) material property parameters including the temperature-dependence of the viscosity (Section 4), the solubility of H_2O, and the diffusivity of H_2O in the glass melt; and (4) the initial concentration of H_2O in the obsidian.

The range of bubble number density found during bubble growth in obsidian in laboratory furnaces by previous workers is $10^9 < N < 10^{11}$ m^{-3} [Ryan et al. 2015; Coumans et al. 2020]; here we select $N = 2.11 \times 10^{10}$ m^{-3} [Coumans et al. 2020]. We use existing constitutive models for the component material parameters of viscosity, H_2O diffusivity, and solubility. For the viscosity, we use the same model [Hess and Dingwell 1996] that is validated in Section 3. For the diffusivity and solubility we use the two models for which there is the best calibration in the context of bubble growth in rhyolitic obsidian [Liu et al. 2005; Zhang and Ni 2010]. We further follow Coumans et al. [2020] in assuming that a pre-nucleated population of very small bubbles exists in the obsidian with initial volume fraction 10^{-4} [this is a technical step, shown to be valid by Coumans et al. 2020].

We solve the Coumans et al. [2020] bubble growth model using the downloadable code they provide. We solve the model in separate individual runs for different temperatures of heat treatment in the range $T_g < T < 1325\,°C$. We repeat this for initial water concentrations 0.1, 0.2, 0.3, 0.4, and 0.5 wt.% initial H_2O, covering the range extant in most natural obsidian lavas [Castro et al. 2014; Wadsworth et al. 2020]. For each run of the model, we output the time at which bubble growth is complete. We note that the model asymptotes to an equilibrium state, and define bubble growth as complete when the modelled volume fraction of bubbles is within 1 % of that of its equilibrium value or when T_g is reached, before we stop the simulation and output the final time of the run. This final time—in seconds—is then the 'bubble growth time' λ.

In Figure 6 we plot our results, showing $\lambda(T)$ for a range of initial water concentrations typical of obsidian in nature. We posit that this represents a guide for makers, such that in order to pre-process their obsidian prior to subsequent glass art steps, they should ensure that their glass is exposed to a value of $T > T_g$ for times $t > \lambda$. Put another way, an artist should ensure that their raw natural glass experiences conditions above the curves in Figure 6. During the making of 'PEDM', the glass was held for 24 hours at 1200 °C, which are conditions in the 'fully degassed' region of Figure 6, indicating that these conditions were sufficient to thoroughly remove the remnant H_2O from the glass, ideal for subsequent artistic making steps.

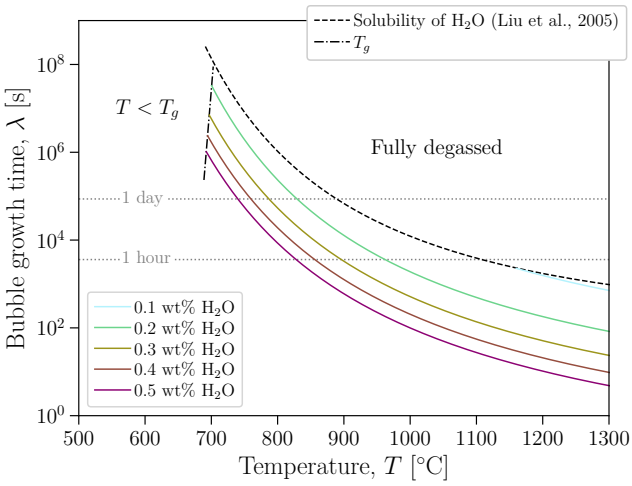

Figure 6: Guide for makers. A quantitative map showing how long obsidian should be held at a given temperature in order to ensure that all the residual water in the obsidian is removed during the growth of bubbles. The individual curves are given as examples and represent solutions to the numerical model for bubble growth in obsidian provided by Coumans et al. [2020] for five different typical dissolved water concentrations in the range 0.1–0.5 wt.%. The field $T < T_g$—demarked by the dash-dot curve—represents temperatures below which obsidian will never soften. The dashed curve represents the interconnection of the output value of λ for the temperature at which the initial H_2O value is at the solubility of H_2O, meaning that at any temperature below that value, bubbles will not form or grow. For example, see 0.1 wt.% H_2O which terminates against the dashed curve at around 1150 °C, such that the blue curve is only valid at temperatures greater than 1150 °C. Therefore, for obsidian with 0.1 wt.% H_2O initially, at temperatures lower than 1150 °C, the obsidian can be used without this pre-processing step. To define the dashed line for a more closely spaced number of values of initial H_2O concentrations than given as solid curves here (to define the dashed curve, we use 0.05–0.2 wt.% closely spaced). The dashed curve also shows that this limit is not relevant for initial H_2O concentrations greater than 0.2 wt.% H_2O, because the solubility temperature is below T_g.

5.1.2 *Casting: Sintering pre-dehydrated obsidian in a mold*

Viscous sintering is a process by which many particles of glass partially or wholly amalgamate or fuse to form a coherent denser body [Rahaman and De Jonghe 1990; Wadsworth et al. 2016]. The porosity—or the volume fraction of the material that is composed of gas ϕ—is the measure of how 'complete' is the sintering process. Initially, the material is a pile or pack of glass particles with a porosity that is represented by the gas-filled space between the particles $\phi \sim 0.5$. But at high temperature, as sintering progresses, the particles fuse together and this gas volume decreases as the particles move and flow together and inward. The bulk volume of the whole material decreases at the expense of the interstitial gas which is pushed out from between the particles, which explains why sinter casting often has to be topped up with new particles mid-sinter [Cummings 1997]. First, we must assess the degree of sintering that occurred in 'PEDM' by assessing the porosity. We can achieve this by measuring its total volume V and its mass m, such that the porosity is given by $\phi = 1 - (m/V)/\rho_0$, where ρ_0 is the density of the glass without any gas phase.

Given the unusual shape and fragility of 'PEDM', we use photogrammetry in order to determine its volume. Two sets of 36 photos, shot with an iPhone 11 (resolution 4032×3024, focal length 4.2 mm, 35-mm, focal length 52, ISO-40, file format .jpg) were used. The iPhone was kept constant on a tripod at approximately 45° above the sample, while 'PEDM' was rotated on a school protractor. Each set of photos corresponds to one full 360° rotation with a photo taken every 10° to ensure a more than 80 % overlap between subsequent photos. We processed the photos with the commercial photogrammetry software `Agisoft™ Metashape`, following the standard software workflow (see the Appendix for specifics). The output is two point-clouds (.ply

Figure 7: 'PEDM' by Alastair Mackie. Top-left: the original piece (as shown in Figure 1E). The other panels show different rotations of the 3D model of the object created using photogrammetry (see text for details). The diameter of the base of the wrist section is 5 cm.

files), which were then scaled, cleaned, and merged in the open-source software `CloudCompare (Version 2.10.2)`. In preparation for an accurate 3D model the single merged point-cloud was then processed to reduce noise, doublet points, and tested for the effect of subsampling. The 3D model was created through the Poisson surface reconstruction (octree level 12) in `CloudCompare` on the final point cloud (2.6×10^6 points) and its subsampled version (2.5×10^4 points). Finally, we calculated the volume from these point-clouds using a calibrated length known on the object (the wrist diameter). The reconstruction of the piece is given in Figure 7.

The workflow described above resulted in a volume for 'PEDM' of $V = 3.024\ (\pm\ 0.011) \times 10^{-5}\ \mathrm{m}^3$. The measured mass of the object is $m = 0.06424$ kg. Assuming the solid glass density is $\rho_0 = 2200\,\mathrm{kg\,m^{-3}}$ [Wadsworth et al. 2019b], this results in a calculated porosity of $\phi = 0.0344\ (\pm\ 0.0035)$, consistent with the thoroughly sintered, smooth nature of the surface of the piece.

In order to tune the porosity of a piece during casting by sintering, the mold must be held at a given temperature for a precise time. Similar to the bubble growth pre-step, this can be predicted *a priori* using an existing model for sintering of obsidian materials [Wadsworth et al. 2019b; 2021]. This sintering model takes as inputs: (1) the particle size of the *frit* used in the casting (or the distribution of the particle sizes if the full distribution is known); and (2) the glass viscosity at the casting temperature, μ. The model also depends on the interfacial tension between the glass melt and the gas between the particles, but this is generally found to be approximately a constant at around $0.3\,\mathrm{N\,m^{-1}}$ [Parikh 1958; Gardner and Ketcham 2011].

As with the bubble growth step, here we aim to provide a map for sinter-casting of obsidian. This allows us to both check the model against the conditions at which 'PEDM' was fabricated, and to provide a general guide for others to use in order to make similar pieces from obsidian. We start from the assumption that the artist is using an obsidian with a particle size around 10^{-4} m diameter and with the pre-bubble-growth step described in Section *5.1.1*. We use a model calibrated for the sintering of angular obsidian glass particles in a similar size range [Wadsworth et al. 2019b; 2021] to contour a sinter-casting map for the times required to reach a given desired porosity for any temperature (Figure 8). We note that the porosity of 'PEDM' ($\phi \approx 0.03$) is the equilibrium value at the end of sintering [Wadsworth et al. 2016] and therefore the fact that the conditions at which the object were made sit above the curves predicted in Figure 8, is consistent with the model prediction.

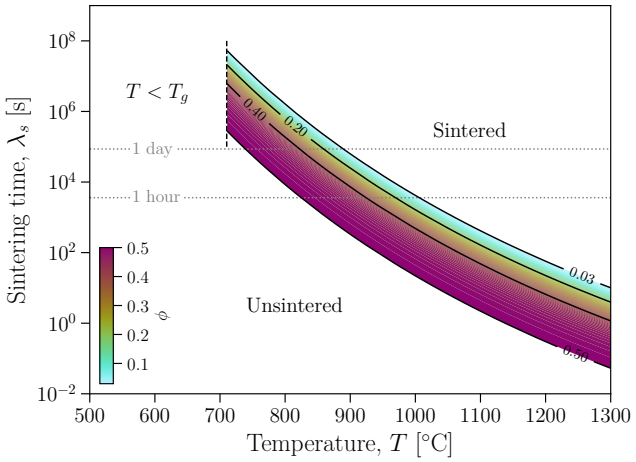

Figure 8: A guide for casting obsidian forms using a sintering technique, showing the time required to reach a given porosity at a given temperature. The map shown here is for 100 μm particles in the obsidian powder, typical of normal dry milling techniques, and is computed using a sintering model [Wadsworth et al. 2016], which was specialized for sintering obsidian particles [Wadsworth et al. 2019b]. Typical initial packing porosities of 0.5 represent the upper porosity bound, whereas the equilibrium porosity of 0.03 represents the lower bound. For casting in the 'unsintered' field, the result will be an unconsolidated powder of obsidian. For casting in the 'sintered' field, the result will be a sheet of glass with a low 0.03 porosity (e.g. Figure 1D). For the conditions of formation of 'PEDM', sinter-casting was performed at 1200 °C for 2 hours, which plots in the 'sintered' field and is consistent with the measured final porosity of $\phi \approx 0.03$, which is the limiting upper value for complete sintering (see Section 5).

5.2 Summary: Using obsidian in glass art

The methods described here for removing gas from obsidian altogether are usable when the pre-processing bubble growth step is performed at the same temperature or a higher temperature than the sinter-casting making step. If this is not the case, then remnant volatiles may remain in the obsidian, and may form bubbles during the second making step.

The full framework described in Section 5.1 is illustrated in Figure 9. The framework described here for producing 'PEDM' is one way to work with obsidian in glass art. However, there are other possible methods for using obsidian, some of which are mentioned in brief here. First, the relatively high temperatures of lamp- or flame-work would allow manipulation of rods and pieces of obsidian. In Figure 10 we show an example test piece of obsidian in lamp-work created by some of the authors. We found that the obsidian is generally less workable (but still workable) than the borosilicate glass often used in lamp-work, consistent with the temperature dependence of viscosity (Figure 3). However, it was possible to fuse pieces obsidian with borosilicate lamp-work, and no significant incompatibility (see Table 1) was found between the obsidian and borosilicate glass (Figure 10). Second, Wadsworth et al. [2021] showed that, if sufficiently small particles are used in sinter-casting, then diffusive loss of H_2O occurs *during* the sinter-casting, and therefore, if a finely crushed sub-*frit* glass powder was used, it is possible that the pre-casting bubble growth step could be skipped. However, this remains untested in casting and has only been validated for small sample cylinders of obsidian at scales of 3 mm diameter [Wadsworth et al. 2021]. There is clearly opportunity for future experimentation with obsidian to refine these recipes for making.

6 Discussion

Here we discuss the use of obsidian in glass art from several viewpoints. First, we discuss the volcanological context and explore the lessons that could be learned from the production of 'PEDM'. Second, we set out the material and process challenges in the use of obsidian or other volcanic materials in glass art. Third, we explore the process or act of making itself and consider the extent to which making with obsidian aligns with current viewpoints about making and makers. Finally, we posit that there are ample opportunities for knowledge-exchange between glass artists and volcano scientists, and that the use of obsidian in glass art can be a case-study in the inter-disciplinary crossovers that are possible here.

6.1 The making of 'PEDM': A microcosm of natural volcanic processes

The making process used by the artist (independently from this study) to create 'PEDM' was not an experiment in volcanology or volcano science; the goal was to make glass art from obsidian materials without the addition of any other components such as a flux. However, in many ways the making steps followed in 'PEDM' (see Section 5) are a microcosm of processes extant in volcanic eruptions. Moreover, the making of 'PEDM' is a direct replica of the processes that are used in volcano science laboratories in order to understand these volcanic phenomena. Indeed, in the first pre-casting bubble growth step designed to dehydrate the obsidian, we use the Coumans et al. [2020] model as a guide for defining the bubble growth time required to reach equilibrium H_2O—termed λ in Figure 6—and in their model validation, Coumans et al. [2020] effectively performed identical experiments using natural obsidian in which obsidian was heated and volume changes induced as a result of bubble growth. Similarly, in analyzing the casting step by sintering, we note the dynamic similarity between the conditions of casting and experiments performed in the validation of sintering theory for obsidian [Wadsworth et al. 2019b; 2021].

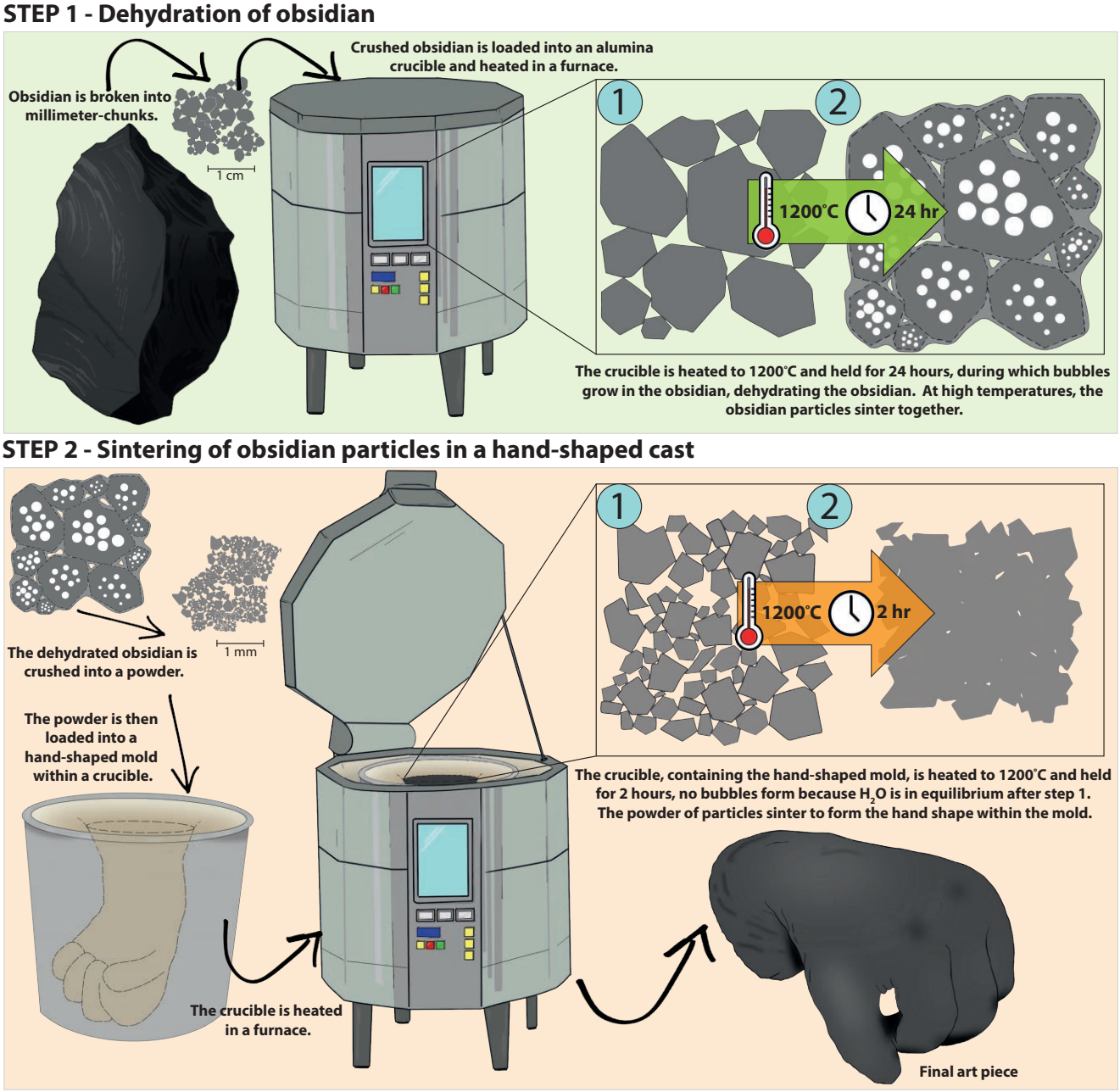

Figure 9: An illustrated workflow for using obsidian in casting, such as in the production of 'PEDM'. Step 1 involves the dehydration of natural obsidian in a pre-processing high-temperature step. Step 2 involves the crushing of the dehydrated obsidian from step 1 in a sinter-casting methodology. See text for details.

In general, magma at depth in the shallow crust - from which obsidian is eventually formed contains substantially higher dissolved H_2O than is found in obsidian at Earth's surface [Wadsworth et al. 2020]. As obsidian-forming magma is moved from those relatively high storage pressures to the surface, the solubility of H_2O drops, dissolved H_2O becomes supersaturated, and bubbles form as a result [Sparks 1978]. This process is 'degassing' (see Section *5.1.1*) and ubiquitous in magmas on Earth, and is directly replicated in the making procedure used to prepare the obsidian for making 'PEDM'. In a volcano, the now bubble-bearing magma then undergoes outgassing via some process, where 'outgassing' refers to a process by which the gas in the bubbles is removed from the magma and ultimately, from the system altogether [Degruyter et al. 2012; von Aulock et al. 2017]. One way to remove the gas from the bubbles is for the magma to fragment under high bubble overpressures, causing the bubbly magma to break apart into fragments of variable size [Alidibirov and Dingwell 1996; Cashman and Scheu 2015; Gonnermann 2015]. Together, bubble formation and growth, followed by magmatic fragmentation, removes dissolved H_2O from the liquid component of

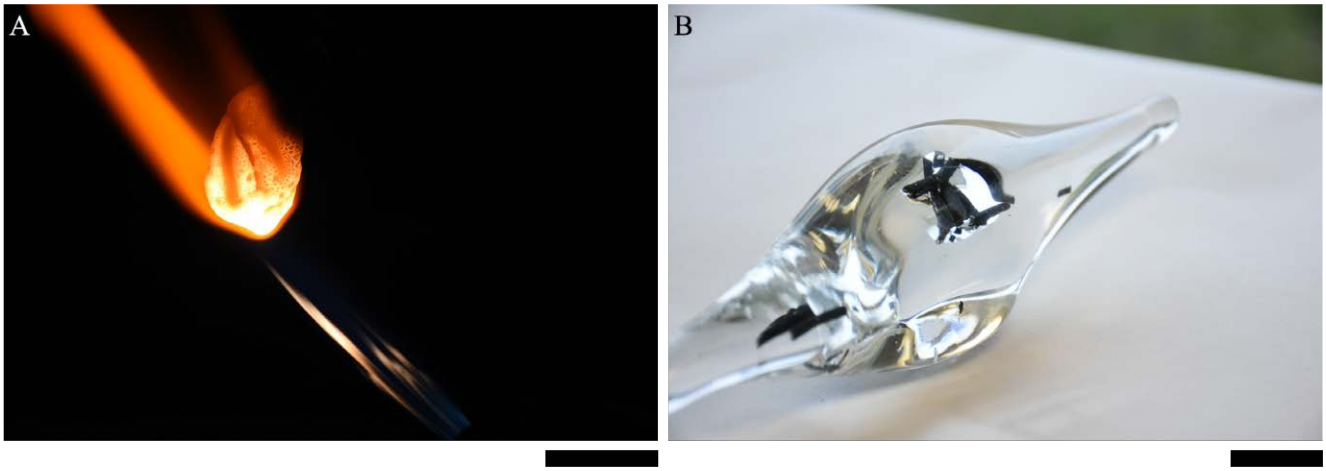

Figure 10: The results of experimentation with volcanic materials at a 2019 'In Vulcan's Forge' workshop held at the National Glass Centre, Sunderland, U.K. [A] An example of lamp- or flame-work with obsidian, showing the surface evidence for bubble formation and growth that is inevitable at high temperatures when a pre-processing step is not taken (c.f. Figure 6). [B] Fragments of basalt trapped in soda-lime-silica glass, showing the apparent lack of evidence for serious incompatibility between volcanic materials and standard glasses (c.f. Table 1), which would manifest as fractures formed during cooling and annealing. The scale bars in the bottom right of the images represent 1 cm, and are indicative (note that [B] is a perspective image).

the magma into a gas (bubbles) component, and then removes the gas altogether, leaving behind the liquid component with now low H_2O values. This is essentially identical to the pre-processing step applied in the making of 'PEDM'. Moreover, this is identical to the method by which obsidian can be rendered usable at high temperatures without running into unwanted bubble formation that can cause issues in glass art production.

Obsidian is typically found as part of lavas or fragments in tephra deposits [Fink 1983; Cabrera et al. 2011; Castro et al. 2012; Tuffen et al. 2021], and not as the blebs of inter-bubble liquid magma that are formed during fragmentation. Wadsworth et al. [2020] suggested that a common formation mechanism of large rhyolite lava bodies that cool to obsidian, is by sintering [Schipper et al. 2021]. Indeed, those authors suggest that it is essentially the degassing, outgassing, fragmentation, and sintering cycle that is required to produce low-H_2O obsidian found on Earth [see Wadsworth et al. 2020, for details of this conceptual cycle/model]. Again, this is the same making procedure used in 'PEDM', where the artist and artist-team sintered, or sinter-cast, the pre-dehydrated chunks of obsidian to produce a more-dense, but low-H_2O, solid obsidian piece (Figure 9). Therefore, we propose that the making procedure of 'PEDM' is a clear example of where the processes extant in volcanoes are dynamically identical to those that are simply necessary for the production of some glass art with obsidian.

The process-focused crossover between glass art making processes, and volcanic phenomena described here is a way-in to thinking about the opportunities that may exist in the space between these two endeavors. With reference to both 'PEDM' itself, but also to the artist-scientist collaborations at the Syracuse Lava Project [Lev et al. 2012; Farrell et al. 2018], Wadsworth et al. [2019a] proposed that both volcanologists and artists have much to gain from "stepping into Vulcan's forge" and working with the magma or magma-like materials. These opportunities do include science communication, education, and outreach endeavors, but clearly there are additional opportunities that may lie closer to the core of the principal goals of both fields. However, truly bilateral engagement between these communities has not been widely explored, or, we would argue, explored to the fullest potential.

6.2 Material and process challenges

A principal finding of this work is that there are challenges associated with working with obsidian, which are not encountered with other glass compositions such as soda-lime-silica or borosilicate glass. We propose that this is part of the reason that obsidian is not used more often in glass art practices. Key popular exemplars of the difficulties of working with obsidian at high temperature are given in the YouTube™ videos from *How To Make Everything* (titles: 'Can You Melt Obsidian and Cast a Sword?'*, 'Melting Dragonglass to Cast an Obsidian Axe'†), in which an unspecified fluxing agent is mixed with crushed obsidian powder prior to melting. Presumably, the flux was thought to be required to render the molten obsidian sufficiently low viscosity for pouring, casting, and manipulating at standard kiln

*https://www.youtube.com/watch?v=CA3lIuN_zVE&t=1s
†https://www.youtube.com/watch?v=uP3a-BweNUc

or furnace temperatures and using standard glass- or metal-working techniques. In a YouTube™ video with a similar aim from *Timon Show* (title: 'Experiment: Obsidian Sword from Lava'* *emphasis removed*), no flux appears to have been used, but rather the starting material may not have been a silicic volcanic rock (see frame at time stamp 0:04 for an image of the starting rock). As such, the glass produced may be a mafic glass. These cases highlight the issue: molten obsidian at the Earth's surface tends to be extremely high viscosity (Figure 3) with a high working temperature for most procedures (Figure 4), presenting challenges to its practical workability without changing its composition via flux.

Similar issues can be found with cold-working obsidian. Obsidian material is not uniform or homogeneous. Julian Charrière's piece 'Thickens, pools, flows, rushes, slows' (Figure 1B) is a key example where the surface texture of the obsidian is clearly heterogeneous. While Charrière was able to cold-work and polish a sequence of smooth bubble-like forms in the obsidian, these heterogeneities often result in inconsistent material strength or internal fractures that make obsidian hard to work and polish.

Our analysis of 'PEDM' and the preparatory experimentation of the artist and artist team who created 'PEDM' demonstrate that challenges associated with excess H_2O can be overcome by a pre-processing step of heating and cooling in order to allow H_2O to form bubbles. Similarly, their making process demonstrates that while pouring, bending, and stretching work that are typically used in glassblowing or hot glass work are not possible at standard working temperatures, casting techniques that exploit the sintering mechanism can be used in kilns or furnaces that can reach the desired target working temperatures (Figure 4) or if long timescales of soak at a given lower temperature are allowed (Figure 9). Therefore 'PEDM' is a case study in how to overcome the hot glass material and process challenges associated with using obsidian without using a chemical fluxing agent and therefore without changing the composition of the obsidian. Similarly, waterjet cutting experimentation presented by the *Waterjet Channel* (title: 'Obsidian with a 60,000 PSI Waterjet – Obsidian Cube Minecraft IRL'†) demonstrates that using precision modern equipment may be a method by which cold-working obsidian can overcome the friability or fracturing challenges associated with heterogeneous obsidian.

Other material challenges may be encountered, such as when attempting to use obsidian as a material with other glasses. The principal issue may surround 'compatibility' (Table 1). To test this and as an 'extension study' reported here by way of discussion, we tried various ways in which obsidian may be utilized in lamp- or flame-work with the borosilicate glass, which has a relatively similar working temperature range (Figure 4). We found no apparent compatibility issues, and were able to enclose obsidian and basaltic glass in borosilicate and soda-lime-silica glass (Figure 10). Indeed, while the working range of temperature between borosilicate and obsidian is similar, the slightly higher working range for fusing and casting processes for the obsidian relative to the borosilicate (Figure 4) renders the obsidian stiffer than the borosilicate at a given temperature. This difference allowed us to boudinage the obsidian piece inside the lower-viscosity flowing borosilicate (Figure 10). If obsidian is compatible with other studio glasses, then this opens up further possibility for mixed-media work and approaches that may be of particular utility where using obsidian alone may not be possible or appropriate because of the high temperatures required.

6.3 The 'Cloud of Unknowing'‡ and the process of making

The process of making an art object invariably results in craft knowledge that cannot always be articulated or passed on. As Polanyi [1966] puts it, "We can know more than we can tell," explaining that the ways of knowing through experience and practice of craft adhere to the practitioner and remain out of reach of the fullest explication. This idea then is that there is some component of a making process that constitutes knowledge held by the maker and the maker only; a material and process knowledge [c.f. McCray 2020]. Bateson [1973] refers to this as knowing from the inside out or knowing by doing and not by formal instruction, such that the maker is taught by the material as much as by an instructor. We use these theoretical ideas of what it is to make something as a starting point for a discussion surrounding how engagement between glass artists and volcanologists can be transformative in terms of knowledge-exchange. Following Polanyi [1966], we ask if experimentation with obsidian in glass art studios may result in volcanologists learning *from* the obsidian directly via experience with the material?

Ingold [2013] sets up a clear distinction between the theorist and the craftsperson, which is encapsulated by the opposition between 'making through thinking' (theorist) and 'thinking through making' (craftsperson). Ingold [2013] argues that seeing art pieces as a compendium of objects to be analyzed renders such analysis disconnected from the making process in terms of the discoveries that can be made *by making*. As Ingold [2013] has it, the scientist's interest is to learn about an object and how it formed or was formed, and

*https://www.youtube.com/watch?v=adXhws3_IEU

†https://www.youtube.com/watch?v=hv3jeGUv9fY

‡'Cloud of Unknowing' is a reference to a piece by co-author Alexandra Carr, in which the cloud is a response to faith and references the artist's own methodology in which instinct drives the process of creating both the concept behind the piece and the piece itself (http://www.alexandracarr.co.uk/cloud-of-unknowing-1). The title draws on a text by the same name (*'Cloude of Unknowyng'* in Middle English) by an anonymous Christian mystic.

to unpick the processes that went on during what is actually a quite separate sequence of correspondences between artist-and-material.

The theorist might look at an art object such as 'PEDM' and map out the *chaîne opératoire*: the sequence of steps involved in a making process. Like Ingold [2013], Deleuze and Guattari [1988] see art objects not as this products of a sequence of discrete steps, but as emerging from a rhizomal flow of motion and thought intertwined. They note that matter is "in movement, in flux, in variation" and that makers follow the matter. Interestingly, they use a high temperature process of making objects in metallurgy as their cornerstone example. Ingold [2013] similarly uses an analogy of solids becoming liquids as metaphor for this material-flow concept of making. In glass art, this is more literal than in many making processes [e.g. Ingold 2013, using the making process of knapping flint as an example]. Bennett [2010] echoes this and sees materials as effable and in the process of becoming other materials; defining this flux as a 'life' in materials that is the reason that artisans and makers can collaborate with it. Put another way, making is perhaps seen best as a journey that changes both the material and the maker themselves.

In this Research Article, we have undertaken the theorist's analysis of *chaîne opértoire*, and therefore it may be true that there is a missing component of the knowledge that can be gained by undertaking the making oneself, that cannot be analyzed or communicated herein. Indeed, Conneller [2012] warns against the application of analytical techniques or models from one field (volcanology) as an analysis for another disparate area of inquiry (art). While, in many ways, the work of the academic volcanologist is that of the theorist as imagined by Ingold [2013], there are components of any experimental science that involve the intuitions and material work to which Ingold [2013] is referring when they discuss making in the most abstract sense of the word. In a volcanology laboratory, solving experimental problems, and producing experimental objects prior to analysis, is surely a form of the same making that is embodied in the 'PEDM' production sequence (Figure 9)? However, Wadsworth et al. [2019a] propose that it is quite a different thing for a volcanologist to step into the glass art studio and work with obsidian more freely than perhaps they ever do in a laboratory.

The opposing view of making is one in which the maker imposes pre-determined form on the natural world in a constructivist sense [Holloway 1992]. When weighing these ideas of making and maker, the example of working with obsidian becomes particularly interesting exactly because it is directly a natural product of the natural world. We posit that there is a range of making approaches exemplified in the examples given in Figure 1, where the axis of the range is the extent to which there has been human engagement in the making. The examples of cold-working from Julian Charrière (Figure 1B) and Eduardo Olbes (Figure 1A) or the hot-working of Matt Durran (Figure 1C) have had relatively little human engagement when compared with 'PEDM' (Figure 1E) and 'Variations on an energetic field' (Figure 1D). In the former examples, there has been little imposition of form [as Holloway 1992, puts it] on the natural obsidian, compared with the latter examples in which the obsidian has been wholly transformed and processed as part of the making. However, in all cases, the material challenges explored herein have been ever-present and in the very undertaking of solving those challenges, we suggest that the 'blueprint' view of making of Holloway [1992] is less tenable than a view described above in which the maker negotiates an outcome with the material and learns from it *through making*.

The argument that there is much to be gained from making as a learning process in and of itself, lead us to conclude that while the technical conclusions of this article are, we hope, of broad utility, there is added value to the volcanologist to experiment creatively with obsidian [Wadsworth et al. 2019a]. We propose that this presents an opportunity to transform the scientist to open up new ways of thinking, laterally and multi-dimensionally. Similarly, it is clear from Section 4 and the processes involved in 'PEDM' that volcanological models can be used to predict the times and temperatures required for 'PEDM' to have been made. Exchanging this knowledge may transform the artist's practice, expedite making, and allow new techniques to be leveraged. In many ways, the playing field of discovery is a level one when it comes to the scaled-up behavior of obsidian. The flow, fracture, and healing behavior of obsidian in nature confounds the expectations of scientists [Tuffen and Dingwell 2005; Wadsworth et al. 2017; Wadsworth et al. 2018; Lamur et al. 2019; Andrews et al. 2021] and renders art-science collaboration mutually beneficial in many respects.

In the discussion undertaken here we have not drawn a clear distinction between the craft aspect of making and the work toward the production of *art*—work that can be different and distinct from the practicalities of *making* itself. Delineating the practices of craft, art, and design (and other such categories of creative making) is fraught and contentious. However, in the context of this discussion, it is worth noting that shifting distinctions are thought to exist in some sense in some cases, and therefore, the role that material experiences play in confronting the maker and changing the maker are perhaps variably applicable depending on the directness of the engagement between the artist and the outcome. For examples where that link is less direct, the conceptual linkages between obsidian, volcanoes, primordial volatiles of the Earth, and the existing cultural links described in Section 1, are all relevant and may be benefits of surmounting the challenges of working with obsidian.

ACKNOWLEDGEMENTS

We are grateful to all the participants of the 2019 'In Vulcan's Forge' workshop, which included research students and staff from both Durham University and the University of Sunderland. We acknowledge support via a Winston Churchill Memorial Trust Fellowship to F.B. Wadsworth, and the *In Vulcan's Forge* project supported by Durham University's Research Seedcorn. We're grateful to Giles Gasper and the Ordered Universe project (https://ordered-universe.com/) for helping to seed this collaborative work at the National Glass Centre 2018. Mohd Zul Hilmi Mayzan is thanked for his help in preparing the obsidian for PEDM. We acknowledge Amy Donovan for editorial handling and guidance, one anonymous reviewer, as well as Ulli Kueppers and Jan Lindsay for reviews that were engaging and constructive, and have led to improvements throughout. We thank Mike Heap for copyediting, and Ery Hughes at Volcanica for production and typesetting. We thank the artists whose work is represented in Figure 1 for permission to share images of their work here.

DATA AVAILABILITY

All data associated with this manuscript are provided as Supplementary Material alongside the online version of this article.

COPYRIGHT NOTICE

REFERENCES

Ackermann, S. and L. Devoy (2012). "'The Lord of the smoking mirror': Objects associated with John Dee in the British Museum". *Studies in History and Philosophy of Science Part A* 43(3), pp. 539–549. DOI: 10.1016/j.shpsa.2011.11.007.

Alidibirov, M. and D. B. Dingwell (1996). "Magma fragmentation by rapid decompression". *Nature* 380(6570), pp. 146–148. DOI: 10.1038/380146a0.

Andrews, G. D. and M. J. Branney (2011). "Emplacement and rheomorphic deformation of a large, lava-like rhyolitic ignimbrite: Grey's Landing, southern Idaho". *Geological Society of America Bulletin* 123(3-4), pp. 725–743. DOI: 10.1130/b30167.1.

Andrews, G. D., S. M. Kenderes, A. G. Whittington, S. L. Isom, S. R. Brown, H. D. Pettus, B. G. Cole, and K. J. Gokey (2021). "The fold illusion: The origins and implications of ogives on silicic lavas". *Earth and Planetary Science Letters* 553, p. 116643. DOI: 10.1016/j.epsl.2020.116643.

Angell, C. A. (1995). "Formation of glasses from liquids and biopolymers". *Science* 267(5206), pp. 1924–1935. DOI: doi.org/10.1126/science.267.5206.1924.

Angell, C. A., K. L. Ngai, G. B. McKenna, P. F. McMillan, and S. W. Martin (2000). "Relaxation in glass-forming liquids and amorphous solids". *Journal of applied physics* 88(6), pp. 3113–3157. DOI: 10.1063/1.1286035.

Bateson, G. (1973). *Steps to an ecology of mind: Collected essays in anthropology, psychiatry, evolution, and epistemology*. Fontana, London.

Bennett, J. (2010). *Vibrant matter: A political ecology of things*. Duke University Press, Durham, NC.

Cabrera, A., R. F. Weinberg, H. M. Wright, S. Zlotnik, and R. A. Cas (2011). "Melt fracturing and healing: A mechanism for degassing and origin of silicic obsidian". *Geology* 39(1), pp. 67–70. DOI: 10.1130/G31355.1.

Casas, A. S., F. B. Wadsworth, P. M. Ayris, P. Delmelle, J. Vasseur, C. Cimarelli, and D. B. Dingwell (2019). "SO_2 scrubbing during percolation through rhyolitic volcanic domes". *Geochimica et Cosmochimica Acta* 257, pp. 150–162. DOI: 10.1016/j.gca.2019.04.013.

Cashman, K. V. and B. Scheu (2015). "Magmatic fragmentation". *The Encyclopedia of Volcanoes*. Ed. by H. Sigurdsson, B. Houghton, S. McNutt, H. Rymer, and J. Styx. Elsevier, pp. 459–471. DOI: 10.1016/B978-0-12-385938-9.00025-0.

Castro, J. M., I. N. Bindeman, H. Tuffen, and C. I. Schipper (2014). "Explosive origin of silicic lava: textural and δD–H_2O evidence for pyroclastic degassing during rhyolite effusion". *Earth and Planetary Science Letters* 405, pp. 52–61. DOI: 10.1016/j.epsl.2014.08.012.

Castro, J. M., B. Cordonnier, H. Tuffen, M. J. Tobin, L. Puskar, M. C. Martin, and H. A. Bechtel (2012). "The role of melt-fracture degassing in defusing explosive rhyolite eruptions at volcán Chaitén". *Earth and Planetary Science Letters* 333, pp. 63–69. DOI: 10.1016/j.epsl.2012.04.024.

Chataigner, C., J.-L. Poidevin, and N. O. Arnaud (1998). "Turkish occurrences of obsidian and use by prehistoric peoples in the Near East from 14,000 to 6000 BP". *Journal of Volcanology and Geothermal Research* 85(1-4), pp. 517–537. DOI: 10.1016/S0377-0273(98)00069-9.

Chivers, M. (2015). "3D Printing Processes Applied to the Creation of Glass Art". *Journal of International Education and Leadership* 5 (1).

Cicconi, M. R. and D. R. Neuville (2019). "Natural Glasses". *Springer Handbook of Glass*. Ed. by J. D. Musgraves, J. Hu, and L. Calvez. Cham: Springer International Publishing, pp. 771–812. DOI: 10.1007/978-3-319-93728-1_22.

Conneller, C. (2012). *An archaeology of materials: substantial transformations in early prehistoric Europe*. Routledge. doi: 10.4324/9780203833728.

Coumans, J., E. Llewellin, F. Wadsworth, M. Humphreys, S. Mathias, B. Yelverton, and J. Gardner (2020). "An experimentally validated numerical model for bubble growth in magma". *Journal of Volcanology and Geothermal Research* 402, p. 107002. doi: 10.1016/j.jvolgeores.2020.107002.

Cummings, K. (1997). *Techniques of kiln-formed glass*. University of Pennsylvania Press.

De Campos, C. and K. Hess (2021). "Geological Glasses". *Encyclopedia of Glass Science, Technology, History, and Culture*. Ed. by P. Richet, R. Conradt, A. Takada, and J. Dyon. Wiley, pp. 815–829. doi: 10.1002/9781118801017.ch7.2.

Degruyter, W., O. Bachmann, A. Burgisser, and M. Manga (2012). "The effects of outgassing on the transition between effusive and explosive silicic eruptions". *Earth and Planetary Science Letters* 349, pp. 161–170. doi: 10.1016/j.epsl.2012.06.056.

Deleuze, G. and F. Guattari (1988). *A thousand plateaus: Capitalism and schizophrenia*. Continuum, London.

Dingwell, D. and D. Virgo (1988). "Viscosities of melts in Na_2O-FeO-Fe_2O_3-SiO_2 system and factors controlling relative viscosities of fully polymerized silicate melts". *Geochimica Cosmochimica Acta* 52(2). doi: 10.1016/0016-7037(88)90095-6.

Dingwell, D. B. (1989). "Shear viscosities of ferrosilicate liquids". *American Mineralogist* 74(9-10), pp. 1038–1044.

Dixon, J., J. Cann, and C. Renfrew (1968). "Obsidian and the origins of trade". *Scientific American* 218(3), pp. 38–47.

Farrell, J., J. Karson, A. Soldati, and R. Wysocki (2018). "Multiple-generation folding and non-coaxial strain of lava crusts". *Bulletin of Volcanology* 80(12), pp. 1–17. doi: 10.1007/s00445-018-1258-5.

Fink, J. H. (1983). "Structure and emplacement of a rhyolitic obsidian flow: Little Glass Mountain, Medicine Lake Highland, northern California". *Geological Society of America Bulletin* 94(3), pp. 362–380. doi: 10.1130/0016-7606(1983)94<362:SAEOAR>2.0.CO;2.

Fluegel, A. (2007). "Glass viscosity calculation based on a global statistical modelling approach". *Glass Technology-European Journal of Glass Science and Technology Part A* 48(1), pp. 13–30.

Fudali, R. and R. Ford (1979). "Darwin glass and Darwin Crater: a progress report". *Meteoritics* 14(3), pp. 283–296. doi: 10.1111/j.1945-5100.1979.tb00504.x.

Gardner, J. E. and R. A. Ketcham (2011). "Bubble nucleation in rhyolite and dacite melts: temperature dependence of surface tension". *Contributions to Mineralogy and Petrology* 162(5), pp. 929–943. doi: /10.1007/s00410-011-0632-5.

Gardner, J. E., F. B. Wadsworth, E. W. Llewellin, J. M. Watkins, and J. P. Coumans (2019). "Experimental constraints on the textures and origin of obsidian pyroclasts". *Bulletin of volcanology* 81(4), pp. 1–15. doi: 10.1007/s00445-019-1283-z.

Gent, A. (1960). "Theory of the parallel plate viscometer". *British Journal of Applied Physics* 11(2), p. 85.

Giordano, D. and D. Dingwell (2003). "Viscosity of hydrous Etna basalt: implications for Plinian-style basaltic eruptions". *Bulletin of Volcanology* 65(1), pp. 8–14. doi: 10.1007/s00445-002-0233-2.

Giordano, D., J. K. Russell, and D. B. Dingwell (2008). "Viscosity of magmatic liquids: a model". *Earth and Planetary Science Letters* 271(1-4), pp. 123–134. doi: 10.1016/j.epsl.2008.03.038.

Gonnermann, H. M. (2015). "Magma fragmentation". *Annual Review of Earth and Planetary Sciences* 43, pp. 431–458. doi: 10.1146/annurev-earth-060614-105206.

Gottsmann, J., D. Giordano, and D. B. Dingwell (2002). "Predicting shear viscosity during volcanic processes at the glass transition: a calorimetric calibration". *Earth and Planetary Science Letters* 198(3-4), pp. 417–427. doi: 10.1016/S0012-821X(02)00522-8.

Halem, H. (1996). *Glass Notes: a reference for the glass artist*. 3rd edition. Franklin Mills Press, Kent, U.K.

Hess, K. and D. B. Dingwell (1996). "Viscosities of hydrous leucogranitic melts: A non-Arrhenian model". *American Mineralogist* 81(9-10), pp. 1297–1300.

Holloway, R. L. (1992). "Culture: A Human Domain". *Current Anthropology* 33, pp. 47–64. doi: 10.1086/204018.

Ingold, T. (2013). *Making: Anthropology, archaeology, art and architecture*. Routledge. doi: 10.4324/9780203559055.

Klein, T. (2018). "Augmented Fauna and Glass Mutations: A Dialogue Between Material and Technique in Glassblowing and 3D Printing". *Leonardo* 51(4), pp. 336–342. doi: 10.1162/leon_a_01640.

Kotz, F., K. Arnold, W. Bauer, D. Schild, N. Keller, K. Sachsenheimer, T. M. Nargang, C. Richter, D. Helmer, and B. E. Rapp (2017). "Three-dimensional printing of transparent fused silica glass". *Nature* 544(7650), pp. 337–339. doi: 10.1038/nature22061.

Kunz, M. L. and R. O. Mills (2021). "A Precolumbian Presence of Venetian Glass Trade Beads in Arctic Alaska". *American Antiquity* 86(2), pp. 395–412. doi: 10.1017/aaq.2020.100.

Lakatos, T., L. Johansson, and B. Simmingskold (1972). "Viscosity temperature relations in the glass system SiO_2-Al_2O_3-Na_2O-K_2O-CaO-MgO in the composition range of technical glasses". *Glass Technology* 13, pp. 88–95.

Lakatos, T. (1976). "Viscosity-Temperature relations in glass composed of SiO_2-Al_2O_3-Na_2O-K_2O-Li_2O-CaO-MgO-BaO-PbO-B_2O_3". *Glasteknisk tidskrift* 31(3), pp. 51–54.

Lamur, A., J. Kendrick, F. Wadsworth, and Y. Lavallée (2019). "Fracture healing and strength recovery in magmatic liquids". *Geology* 47, pp. 195–198. DOI: 10.1130/G45512.1.

Lev, E., M. Spiegelman, R. Wysocki, and J. Karson (2012). "Investigating lava flow rheology using video analysis and numerical flow models". *Journal of Volcanology and Geothermal Research* 247-248, pp. 62–73. DOI: 10.1016/j.jvolgeores.2012.08.002.

Liu, Y., Y. Zhang, and H. Behrens (2005). "Solubility of H_2O in rhyolitic melts at low pressures and a new empirical model for mixed H_2O–CO_2 solubility in rhyolitic melts". *Journal of Volcanology and Geothermal Research* 143, pp. 219–235. DOI: 10.1016/j.jvolgeores.2004.09.019.

Lukens, M. G. (1965). "Medieval Islamic Glass". *The Metropolitan Museum of Art Bulletin* 23(6), pp. 198–208. DOI: 10.2307/3258166.

Martin, G. R. R. (1996). *A game of thrones*. Bantam.

Martinez, L.-M. and C. Angell (2001). "A thermodynamic connection to the fragility of glass-forming liquids". *Nature* 410(6829), pp. 663–667. DOI: 10.1038/35070517.

McCray, W. P. (2020). *Making art work: How Cold War engineers and artists forged a new creative culture*. MIT Press.

Mitchell, J. (2015). "Precision Air Entrapment through Applied Digital and Kiln Technologies: A New Technique in Glass Art". PhD thesis. University of Sunderland.

Mouly, R. J. (1969). "Systems engineering in the glass industry". *IEEE Transactions on Systems Science and Cybernetics* 5(4), pp. 300–312. DOI: 10.1109/TSSC.1969.300223.

Napolitano, A. and E. G. Hawkins (1970). *Viscosity of a standard borosilicate glass*. Vol. 260. 23. US Government Printing Office. DOI: 10.6028/jres.068a.042.

Newcomb, S. (2009). *The world in a crucible: laboratory practice and geological theory at the beginning of geology*. Vol. 449. Geological Society of America.

O'Connor, E. (2007). "Embodied knowledge in glassblowing: the experience of meaning and the struggle towards proficiency". *The Sociological Review* 55, pp. 126–141. DOI: 10.1111/j.1467-954X.2007.00697.x.

Parikh, N. (1958). "Effect of atmosphere on surface tension of glass". *Journal of the American Ceramic Society* 41(1), pp. 18–22. DOI: 10.1111/j.1151-2916.1958.tb13497.x.

Petrie, K. (2019). "On Glass, in Glass, of Glass: Some Developments in the Combination of Glass and Printmaking". *Arts*. Vol. 8. 1. Multidisciplinary Digital Publishing Institute, p. 21. DOI: 10.3390/arts8010021.

Pocklington, H. (1940). "Rough measurement of high viscosities". *Mathematical Proceedings of the Cambridge Philosophical Society*. Vol. 36. 4. Cambridge University Press, pp. 507–508. DOI: 10.1017/S0305004100017564.

Polanyi, M. (1966). *The Tacit Dimension*. Routeledge and Kegan Paul, London.

Prousevitch, A., D. Sahagian, and A. Anderson (1993). "Dynamics of diffusive bubble growth in magmas: Isothermal case". *Journal of Geophysical Research: Solid Earth* 98(B12), pp. 22283–22307. DOI: 10.1029/93JB02027.

Rahaman, M. N. and L. C. De Jonghe (1990). "Sintering of spherical glass powder under a uniaxial stress". *Journal of the American Ceramic Society* 73(3), pp. 707–712. DOI: 10.1111/j.1151-2916.1990.tb06576.x.

Ryan, A. G., J. K. Russell, K.-U. Hess, A. B. Phillion, and D. B. Dingwell (2015). "Vesiculation in rhyolite at low H_2O contents: A thermodynamic model". *Geochemistry, Geophysics, Geosystems* 16(12), pp. 4292–4310. DOI: 10.1002/2015GC006024.

Saubin, E., B. Kennedy, H. Tuffen, M. Villeneuve, J. Davidson, and S. Burchardt (2019). "Comparative field study of shallow rhyolite intrusions in Iceland: Emplacement mechanisms and impact on country rocks". *Journal of Volcanology and Geothermal Research* 388, p. 106691. DOI: 10.1016/j.jvolgeores.2019.106691.

Schipper, C. I., J. M. Castro, B. M. Kennedy, H. Tuffen, J. Whattam, F. B. Wadsworth, R. Paisley, R. H. Fitzgerald, E. Rhodes, L. N. Schaefer, et al. (2021). "Silicic conduits as supersized tuffisites: Clastogenic influences on shifting eruption styles at Cordón Caulle volcano (Chile)". *Bulletin of Volcanology* 83(2), pp. 1–22. DOI: 10.1007/s00445-020-01432-1.

Schmid, E. (1998). *Beginning Glassblowing*. Glass Mountain Press, Bellingham, Washington.

Seropian, G., B. M. Kennedy, J. E. Kendrick, Y. Lavallée, A. R. Nichols, F. W. Von Aulock, D. B. Dingwell, K.-U. Hess, A. Lamur, J. Schauroth, et al. (2022). "Vesiculation of rhyolitic melts under oscillatory pressure". *Frontiers in Earth Science*, p. 219. DOI: 10.3389/FEART.2022.812311.

Sparks, R. S. J. (1978). "The dynamics of bubble formation and growth in magmas: a review and analysis". *Journal of Volcanology and Geothermal Research* 3(1-2), pp. 1–37. DOI: 10.1016/0377-0273(78)90002-1.

Stern, E. and B. Schlick-Nolte (1994). *Early Glass of the Ancient World: 1600 B.C.–A.D. 50 : Ernesto Wolf Collection*. Distributed Art Pub Incorporated.

Tobolsky, A. and R. Taylor (1963). "Viscoelastic properties of a simple organic glass". *The Journal of Physical Chemistry* 67(11), pp. 2439–2442. DOI: 10.1021/j100805a044.

Tuffen, H. and J. M. Castro (2009). "The emplacement of an obsidian dyke through thin ice: Hrafntinnuhryggur, Krafla Iceland". *Journal of Volcanology and Geothermal Research* 185(4), pp. 352–366. DOI: 10.1016/j.jvolgeores.2008.10.021.

Tuffen, H. and D. Dingwell (2005). "Fault textures in volcanic conduits: evidence for seismic trigger mechanisms during silicic eruptions". *Bulletin of Volcanology* 67(4), pp. 370–387. doi: 10.1007/s00445-004-0383-5.

Tuffen, H., S. Flude, K. Berlo, F. Wadsworth, and J. Castro (2021). "Obsidian". *Encyclopedia of Geology*. Ed. by D. Alderton and S. A. Elias. 2nd edition. Oxford: Academic Press, pp. 196–208. doi: https://doi.org/10.1016/B978-0-12-409548-9.12527-8.

Volf, M. B. (1961). *Technical glasses*. Tech. rep.

Von Aulock, F. W., B. M. Kennedy, A. Maksimenko, F. B. Wadsworth, and Y. Lavallée (2017). "Outgassing from open and closed magma foams". *Frontiers in Earth Science* 5, p. 46. doi: 10.3389/feart.2017.00046.

Wadsworth, F. B., T. Witcher, J. Vasseur, D. B. Dingwell, and B. Scheu (2017). "When Does Magma Break?" *Volcanic Unrest: From Science to Society*. Ed. by J. Gottsmann, J. Neuberg, and B. Scheu. Cham: Springer International Publishing, pp. 171–184. doi: 10.1007/11157_2017_23.

Wadsworth, F. B., E. W. Llewellin, C. Rennie, and C. Watkinson (2019a). "In Vulcan's forge". *Nature Geoscience* 12(1), pp. 2–3. doi: 10.1038/s41561-018-0283-5.

Wadsworth, F. B., E. W. Llewellin, J. Vasseur, J. E. Gardner, and H. Tuffen (2020). "Explosive-effusive volcanic eruption transitions caused by sintering". *Science advances* 6(39), eaba7940. doi: 10.1126/sciadv.aba7940.

Wadsworth, F. B., J. Vasseur, E. W. Llewellin, R. J. Brown, H. Tuffen, J. E. Gardner, J. E. Kendrick, Y. Lavallée, K. J. Dobson, M. J. Heap, et al. (2021). "A model for permeability evolution during volcanic welding". *Journal of Volcanology and Geothermal Research* 409, p. 107118. doi: 10.1016/j.jvolgeores.2020.107118.

Wadsworth, F. B., J. Vasseur, E. W. Llewellin, J. Schauroth, K. J. Dobson, B. Scheu, and D. B. Dingwell (2016). "Sintering of viscous droplets under surface tension". *Proceedings of the Royal Society A: Mathematical, Physical and Engineering Sciences* 472(2188), p. 20150780. doi: 10.1098/rspa.2015.0780.

Wadsworth, F. B., J. Vasseur, J. Schauroth, E. W. Llewellin, K. J. Dobson, T. Havard, B. Scheu, F. W. von Aulock, J. E. Gardner, D. B. Dingwell, et al. (2019b). "A general model for welding of ash particles in volcanic systems validated using in situ X-ray tomography". *Earth and Planetary Science Letters* 525, p. 115726. doi: 10.1016/j.epsl.2019.115726.

Wadsworth, F. B., T. Witcher, C. E. Vossen, K.-U. Hess, H. E. Unwin, B. Scheu, J. M. Castro, and D. B. Dingwell (2018). "Combined effusive-explosive silicic volcanism straddles the multiphase viscous-to-brittle transition". *Nature communications* 9(1), pp. 1–8. doi: 10.1038/s41467-018-07187-w.

Weaver, J., Y. Lavallée, M. Ashraf, J. E. Kendrick, A. Lamur, J. Schauroth, and F. B. Wadsworth (2022). "Vesiculation and densification of pyroclasts: A clast-size dependent competition between bubble growth and diffusive outgassing". *Journal of Volcanology and Geothermal Research*, p. 107550. doi: 10.1016/j.jvolgeores.2022.107550.

Wilding, M., S. Webb, and D. B. Dingwell (1996). "Tektite cooling rates: calorimetric relaxation geospeedometry applied to a natural glass". *Geochimica et cosmochimica acta* 60(6), pp. 1099–1103. doi: 10.1016/0016-7037(96)00010-5.

Zhang, Y. and H. Ni (2010). "Diffusion of H, C, and O components in silicate melts". *Reviews in Mineralogy and Geochemistry* 72(1), pp. 171–225. doi: 10.2138/rmg.2010.72.5.

Appendix

Here we describe the methods used to get the volume of PEDM presented in the main-text. In Table A1, we describe the workflow steps involved in going from a sequence of photos to a final 3D volume-calibrated mesh. The terminology used in Table A1 is specific to the software used (`Agisoft Metashape` and `CloudCompare`) and simply details the settings applied in our use-case. Then in Figure A1, we show some of the results from some of the steps given in Table A1.

Table A1: Workflow for volume analysis using collections of images.

1. Using `Agisoft Metashape`		
Workflow step	Parameters	Result/output
Import photos		36 photos (2× chunk)
Photo quality estimate		0.77–0.83
Align photos	Accuracy: Highest	Tie points
	Generic pre-selection: Yes	Chunk 1: 4150 pts
	Reference pre-selection: Yes	Chunk 2: 4559 pts
	Key point limit: 100,000	
	Tie-point limit: 10,000	
	Adaptive camera model fitting: No	
Build point cloud	Quality: Ultra high	
	Filtering mode: Aggressive	
Cleaning of sparse point cloud	Gradual selection tool	Dense point cloud
	Reconstruction of uncertainty: 10	Chunk 1: 21,393,779 pts
	Projection accuracy: 10	Chunk 2: 23,109,381 pts
	Reprojection error: 1.01	
Data export		.ply files (2x)
2. Using `CloudCompare v2.10.2`		
Workflow step	Parameters	Result/output
Scaling, merging, cleaning of input .ply files		
Remove duplicate points	Min distance between points 1E-12 (default)	6.7M pts
Noise filter	Neighbour sphere radius 6.1E-6 m	3M pts
	Relative max error: 1	
	Remove isolated points: check	
Statistical outlier removal	Number of points for mean-distance estimate: 6 (default)	2.6M pts
	Standard deviation multiplier threshold: 1 (default)	
Subsampling	Space: 0.0005	25k pts
Poisson surface reconstruction	Octree depth: 12	3D model (mesh) with 21M faces (from 2.6M pts) or 83k faces (from 25k pts)

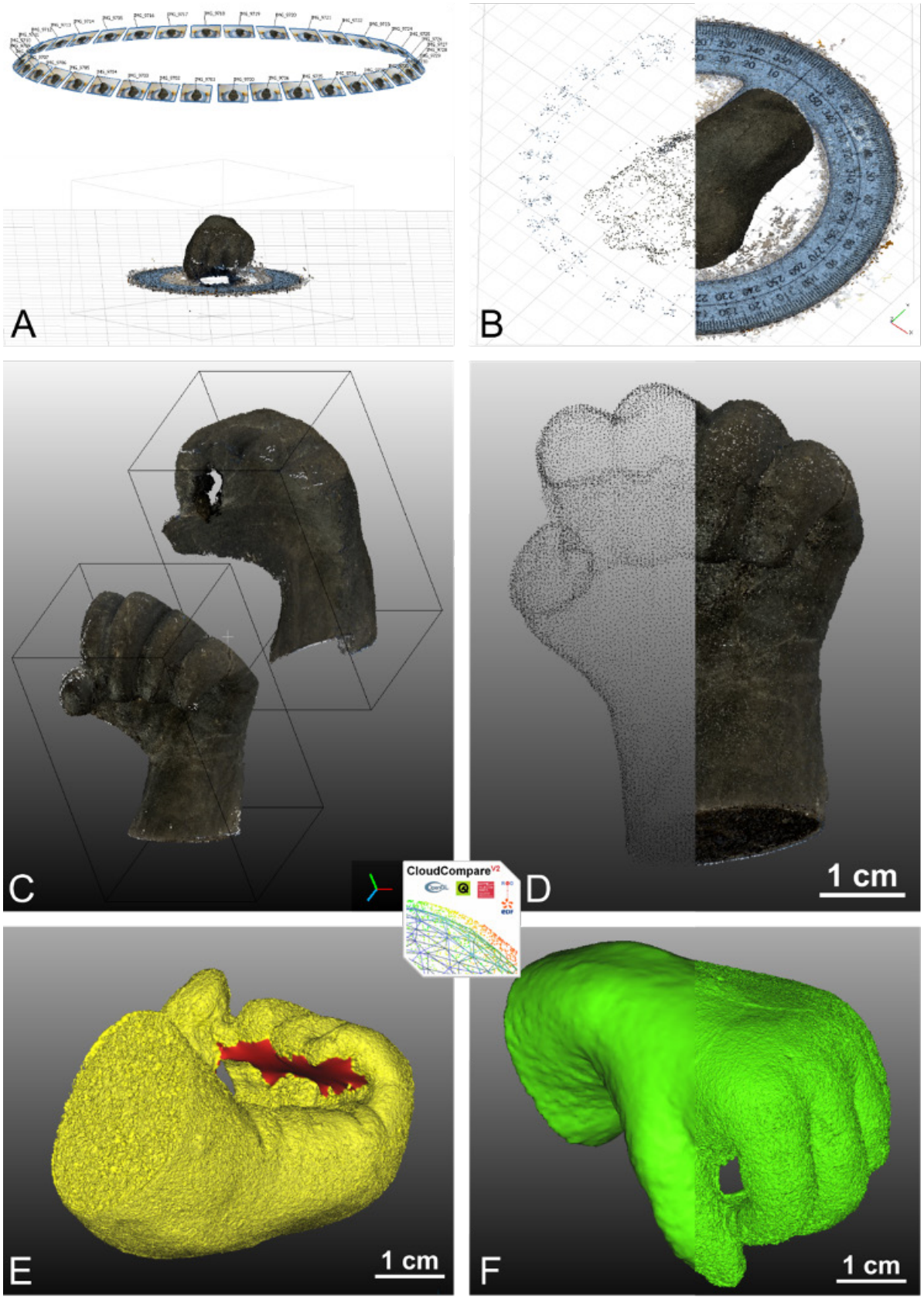

Figure A1: [A] Photo location and dense point cloud in `Agisoft Metashape`. [B] Tie points (feature points) as sparse point cloud (left), dense point cloud (right) in `Agisoft Metashape`. [C] Upper and lower point cloud before merging in `CloudCompare`. [D] Subsampled point cloud (left) with ~10 % of the number of points from the original (right). [E] Red highlights the parts with strong interpolation due to no points/no photo coverage. [F] Difference in roughness of the 3D models (mesh) originating from the subsampled point cloud (left) and the original point cloud (right).